Table 2
Primer pairs used for RT-PCR

Gene	GeneBank accession number		Primer sequence	Product (bp)
ACC	NM_133360	F	5′-GGGCACAGACCGTGGTAGTT-3′	105
		R	5′-CAGGATCAGCTGGGATACTGAGT-3′	
ApoB	NM_009693	F	5′-TCACCCCCGGGATCAAG-3′	85
		R	5′-TCCAAGGACACAGAGGGCTTT-3′	
AOX	NM_015729	F	5′-TGGTATGGTGTCGTACTTGAATGAC-3′	145
		R	5′-AATTTCTACCAATCTGGCTGCAC-3′	
FAS	NM_007988	F	5′-ATCCTGGAACGAGAACACGATCT-3′	140
		R	5′-AGAGACGTGTCACTCCTGGACTT-3′	
FAT	NM_007643	F	5′-CCAAATGAAGATGAGCATAGGACAT-3′	87
		R	5′-GTTGACCTGCAGTCGTTTTGC-3′	
FATP	NM_011977	F	5′-ACCACCGGGCTTCCTAAGG-3′	80
		R	5′-CTGTAGGAATGGTGGCCAAAG-3′	
GAPDH	M32599	F	5′-TGCACCACCAACTGCTTAG-3′	177
		R	5′-GGATGCAGGGATGATGTTCTG-3′	
L-FABP	NM_017399	F	5′-GCAGAGCCAGGAGAACTTTGAG-3′	121
		R	5′-TTTGATTTTCTTCCCTTCATGCA-3′	
MCAD	NM_007382	F	5′-TGCTTTTGATAGAACCAGACCTACAGT-3′	128
		R	5′-CTTGGTGCTCCACTAGCAGCTT-3′	
MTP	NM_008642	F	5′-GAGCGGTCTGGATTTACAACG-3′	72
		R	5′-GTAGGTAGTGACAGATGTGGCTTTTG-3′	
PPARα	NM_011144	F	5′-CCTCAGGGTACCACTACGGAGT-3′	69
		R	5′-GCCGAATAGTTCGCCGAA-3′	

F, forward sequence; R, reverse sequence.

cell division, as revealed by the expression of cell cycle regulators such as cyclin D1 and CDK4. Furthermore, there is little change in apoptosis, which, under normal circumstances, would remove damaged cells capable of undergoing transformation. Thus, under these conditions, it is plausible that some aberrant hepatocytes do not undergo apoptosis and develop into HCC.

It is well known that chronic activation of PPARα is associated with hepatocarcinogenesis in mice exposed to peroxisome proliferators or in mice lacking AOX expression. The common clinicopathological characteristics of HCC in these mice are multicentric HCC (20, 22, 36, 37), the well-differentiated appearance of HCC including trabecular features and often a "nodule-in-nodule" pattern (22, 36, 37), and no evidence of fibrosis or cirrhosis in the nonneoplastic liver parenchyma (22, 36), similar to that observed in *Ppara*$^{+/+}$:HCVcpTg mice. However, mice chronically exposed to peroxisome proliferators are clearly distinct from *Ppara*$^{+/+}$:HCVcpTg mice in that they have normal mitochondrial organization, increased mitochondrial β-oxidation activity, and no steatosis (16, 36). AOX-null mice are also different from *Ppara*$^{+/+}$:HCVcpTg mice with respect to mitochondrial structure (22). These detailed comparisons between the 3 mouse models reveal the importance of mitochondrial abnormalities in the pathogenesis of HCV-related diseases.

PPARα is known to regulate the hepatic expression of many proteins associated with fatty acid and triglyceride metabolism, cell division and apoptosis, oxidative stress generation and degradation, and so forth (15, 16, 20, 21, 24–26); therefore, complete deletion of the PPARα gene from mice might cause hitherto unknown influences on the pathways involved in the development of hepatic steatosis and HCC. To consider these unknown effects, *Ppara*$^{+/-}$:HCVcpTg mice were adopted in the current study. Surprisingly, almost all results from *Ppara*$^{+/-}$:HCVcpTg mice were similar to those from *Ppara*$^{-/-}$:HCVcpTg mice, which demonstrates that the presence of functional PPARα itself is not a prerequisite for the occurrence of steatosis and HCC induced by the HCV core protein. Moreover, a comparison between *Ppara*$^{+/-}$:HCVcpTg and *Ppara*$^{+/+}$:HCVcpTg mice uncovered an unexpected and important fact that the core protein–dependent pathological changes do not appear without significant activation of PPARα. Thus, it is not the presence of PPARα per se, but rather a high level of PPARα activation that seems to be essential for the development of HCV core protein–induced steatosis and HCC.

To reinforce the abovementioned hypothesis, *Ppara*$^{+/-}$ and *Ppara*$^{+/-}$:HCVcpTg mice were treated with an exogenous PPAR agonist, clofibrate, for 24 months. In *Ppara*$^{+/-}$ mice, long-term clofibrate treatment caused a certain level of persistent PPARα activation and a low incidence of HCC. Interestingly, in *Ppara*$^{+/-}$:HCVcpTg mice, clofibrate treatment induced more intensive PPARα activation and HCC at a much higher incidence, accompanied by damaged mitochondrial outer membranes, severe steatosis, and decreased mitochondrial β-oxidation activity. The results from the clofibrate-treated *Ppara*$^{+/-}$:HCVcpTg mice were similar to those of the *Ppara*$^{+/+}$:HCVcpTg mice not treated with clofibrate. Therefore, these findings further support the concept that a long-term and high level of PPARα activation is necessary for steatogenesis and hepatocarcinogenesis in HCVcpTg mice and emphasize the significant role of the HCV core protein as a PPARα coactivator in vivo.

A pulse-chase experiment showed that PPARα was stabilized in hepatocyte nuclei in mice expressing the HCV core protein. Many nuclear receptors, including PPARα and RXRα, are known to be degraded by the ubiquitin-proteasome system (38), which plays an important role in modulating the activity of nuclear receptors. Further studies will be needed to clarify whether the core protein influences the ubiquitin-proteasome pathway.

Recent studies have shown conflicting result, i.e., that PPARα was downregulated in the livers of chronic hepatitis C patients (39, 40). Although the association between PPARα function and chronic HCV infection remains a matter of controversy in humans, the changes observed in the transgenic mice resemble in many ways the clinicopathological features of chronically HCV-infected patients; both show a high frequency of accompanying steatosis (10, 40, 41), increased accumulation of carbon 18 monounsaturated fatty acids in the liver (42), mitochondrial dysfunction (43), increased insulin resistance (44) and oxidative stress (45, 46), male-preferential (2) and multicentric occurrence of HCC (47, 48), and the well-differentiated appearance of HCC, including trabecular features and often a "nodule-in-nodule" pattern (47, 48). Thus, it is postulated that the mechanism of steatogenesis and hepatocarcinogenesis we proposed may partially apply to patients with chronic HCV infection. If so, therapeutic interventions to alleviate persistent and excessive PPARα activation might be beneficial in the prevention of HCC. To clarify the exact relationship between PPARα activation and HCV-induced hepatocarcinogenesis in humans, further

experiments using noncancerous liver tissues obtained from HCV-related HCC patients and using mice carrying human PPARα and HCV core protein genes are needed.

In conclusion, we clarified for the first time that persistent and potent PPARα activation is absolutely required for the development of severe steatosis and HCC induced by HCV core protein. In addition, we uncovered paradoxical and specific functions of PPARα in the mechanism of steatogenesis mediated by the core protein. Our results offer clues in the search for novel therapeutic and nutritional management options, especially with respect to neutral lipids, for chronically HCV-infected patients.

Methods

Mice. The generation of HCVcpTg mice and *Ppara*$^{-/-}$ mice was described previously (7, 24, 49). Male HCVcpTg mice and female *Ppara*$^{-/-}$ mice were mated, and F1 mice bearing the HCV core protein gene were intercrossed to produce F2 mice. *Ppara*$^{+/+}$, *Ppara*$^{+/-}$, and *Ppara*$^{-/-}$ mice bearing the HCV core protein gene, designated as *Ppara*$^{+/+}$:HCVcpTg, *Ppara*$^{+/-}$:HCVcpTg, and *Ppara*$^{-/-}$:HCVcpTg mice, in the F4 generation were subjected to serial analyses. Because HCC develops preferentially in male HCVcpTg mice (9), male mice were analyzed. Age-matched male *Ppara*$^{+/+}$ mice without the core protein gene were used as controls. For identifying genotypes, genomic DNA was isolated from mouse tails and amplified by PCR. Primer pairs were designed as described elsewhere: 5′-GCCCACAGGACGTTAAGTTC-3′ and 5′-TAGTTCACGCCGTCCTCCAG-3′ for the HCV core gene (7) and 5′-CAGAGCAACCATCCAGATGA-3′ and 5′-AAACGCAACGTAGAGTGCTG-3′ for the PPARα gene (24). Amplified alleles for HCV core and PPARα genes were 460 and 472 base pairs, respectively. Five mice per cage were fed a routine diet and were kept free of specific pathogens according to institutional guidelines. For the clofibrate treatment experiments, 2-month-old male *Ppara*$^{+/+}$ and *Ppara*$^{+/-}$:HCVcpTg mice were randomly divided into 2 groups (n = 20 in each group) and were fed either a routine diet or one containing 0.05% (w/w) clofibrate (Wako Pure Chemicals Industries) for 24 months. All mice were killed by cervical dislocation before their livers were excised. If a hepatic tumor was present, the tumor was removed and subjected to histological analysis, and the remaining liver tissues were used for biochemical analyses. All animal experiments were conducted in accordance with animal study protocols outlined in the *Guide for the Care and Use of Laboratory Animals* prepared by the National Academy of Sciences and approved by the Shinshu University School of Medicine.

Preparation of nuclear, mitochondrial, and cytosolic fractions. Approximately 400 mg of liver tissue was minced on ice and transferred to 10% (w/v) isolation buffer (250 mM sucrose in 10 mM Tris-HCl [pH 7.4] and 0.5 mM EGTA and 0.1% bovine serum albumin [pH 7.4]). The samples were gently homogenized by 10–20 strokes with a chilled Dounce homogenizer (Wheaton) and loose-fitting pestle. The homogenate was centrifuged at 500 × *g* for 5 min at 4°C. The supernatant was retained, and the resulting pellet was resuspended with isolation buffer and centrifuged at 4,500 *g* for 10 min at 4°C. The pellet fraction was suspended again and centrifuged at 20,000 × *g* for 1 h at 4°C, and the resulting pellet was used as the nuclear fraction. The combined supernatant fractions were centrifuged at 7,800 × *g* for 10 min at 4°C to obtain a crude mitochondria pellet. This pellet was resuspended with isolation buffer, centrifuged at 7,800 × *g* for 10 min at 4°C, and used as the mitochondrial fraction. Finally, all supernatant fractions were collected and centrifuged at 20,000 × *g* for 30 min at 4°C, and the resulting supernatant was used as the cytosolic fraction.

Immunoblot analysis. Protein concentrations were measured colorimetrically with a BCA Protein Assay kit (Pierce). For the analysis of fatty acid–metabolizing enzymes, hepatocyte mitochondrial fractions or whole-liver lysates (20 μg protein) were subjected to 10% SDS-PAGE (16). For analysis of PPARα, nuclear fractions (100 μg protein) were used. For analysis of other proteins, whole lysates or cytosolic fractions (50 μg protein) were subjected to electrophoresis. After electrophoresis, the proteins were transferred to nitrocellulose membranes, which were incubated with the primary antibody and then with alkaline phosphatase-conjugated goat anti-rabbit or anti-mouse IgG. Antibodies against HCV core protein, fatty acid–metabolizing enzymes, CYP4A1, catalase, and PPARα were described previously (9, 16, 24, 50). Antibodies against other proteins were purchased commercially: cytochrome *c* antibody from BD Transduction Laboratories and other antibodies from Santa Cruz Biotechnology. The band of actin or histone H1 was used as the loading control. The band intensity was measured densitometrically, normalized to that of actin or histone H1, and subsequently expressed as fold changes relative to that of *Ppara*$^{+/+}$ nontransgenic mice.

Analysis of mRNA. Total liver RNA was extracted using an RNeasy Mini Kit (Qiagen), and cDNA was generated by SuperScript II reverse transcriptase (Gibco BRL). Quantitative RT-PCR was performed using a SYBR green PCR kit and an ABI Prism 7700 Sequence Detection System (Applied Biosystems). The primer pairs used for RT-PCR are shown in Table 2. The mRNA level was normalized to the GAPDH mRNA level and subsequently expressed as fold changes relative to that of *Ppara*$^{+/+}$ nontransgenic mice.

Light microscopy and immunohistochemical analysis. Small blocks of liver tissue from each mouse were fixed in 10% formalin in phosphate-buffered saline and embedded in paraffin. Sections (4 μm thick) were stained with hematoxylin and eosin. For immunohistochemical localization of PCNA and 8-OHdG, other small blocks of liver tissue were fixed in 4% paraformaldehyde in phosphate-buffered saline. Sections (4 μm thick) then were affixed to glass slides and incubated overnight with mouse monoclonal antibodies against PCNA (1:100 dilution; Santa Cruz) or 8-OHdG (1:10 dilution; Japan Institute for the Control of Aging). Sections were immunostained using EnVision+ kit, with 3,3′-diaminobenzidine as a substrate (DAKO). Hepatocytes positive for PCNA or 8-OHdG were examined in 10 randomly selected ×400 microscopic fields per section. Two-thousand hepatocytes were examined for each mouse, and the number of immunostained hepatocyte nuclei was expressed as a percentage.

Assessment of hepatocyte apoptosis. TUNEL assay was performed using a MEBSTAIN Apoptosis Kit II (Medical & Biological Laboratories). Two thousand hepatocytes were examined for each mouse, and the number of TUNEL-positive hepatocytes was expressed as a percentage.

Pulse-label and pulse-chase experiments. Parenchymal hepatocytes were isolated by the modified *in situ* perfusion method (51). After perfusion with 0.05% collagenase solution (Wako), the isolated hepatocytes were washed 3 times by means of differential centrifugation and the dead cells were removed by density-gradient centrifugation at 500 *g* for 3 min at 4°C on Percoll (Amersham Pharmacia Biotech). The live hepatocytes were washed and suspended in William's E medium containing 5% FBS. When the viability of the isolated hepatocytes exceeded 85% as determined by the trypan blue exclusion test, the following experiments were conducted. The isolated hepatocytes were washed twice and incubated in methionine-free medium containing 5% dialyzed FBS for 1 h at 37°C. The medium was replaced with the same medium containing 300 mCi/ml of [^{35}S]methionine (Amersham Pharmacia Biotech). After a 3-h incubation, the labeled medium was exchanged for the standard medium, and the preparation was chased for 3, 6, or 12 h. The labeled cells were washed, homogenized, and centrifuged at 800 *g* for 5 min at 4°C to obtain a crude nucleus pellet. This pellet was resuspended with isolation buffer and centrifuged at 20,000 *g* for 1 h at 4°C to prepare the nuclear fraction. The levels of radioactivity in the homogenates of the pulse-labeled preparations were similar between the transgenic and the nontransgenic mice, which suggested that the [^{35}S]methionine uptake capacity in the former hepatocytes was similar to that in the latter. The nuclear fraction was lysed in RIPA buffer (10 mM Tris-HCl, pH 7.4; 0.2% sodium deoxycholate, 0.2% Nonidet P-40, 0.1% SDS,

0.25 mM PMSF, and 10 mg/ml aprotinin). The lysate was incubated for 3 h at 4°C with purified anti-PPARα antibody. The immune complexes were precipitated with *Staphylococcus aureus* protein A bound to agarose beads. After the precipitates had been washed in RIPA buffer, the labeled proteins were resolved by 10% SDS-PAGE and visualized by autoradiography.

Analysis of fatty acid uptake ability. Assays for fatty acid uptake were carried out according to a method reported by Graulet et al. (52) with minor modifications. Briefly, 3 mice in each group were fasted overnight. Livers were removed quickly, rinsed in ice-cold saline solution, and cut into 500-μm thick slices with an Oxford Vibratome (Oxford Laboratories). Approximately 150 mg of fresh liver (6–8 liver slices) was placed on stainless steel grids positioned in a 25-ml flask equipped with suspended plastic center wells (Kontes) and incubated in RPMI-1640 medium (Sigma-Aldrich) devoid of fatty acids for 2 h at 37°C. The medium was then replaced with fresh RPMI-1640 medium supplemented with an antibiotic-antimycotic cocktail and 0.8 mM [1-^{14}C]palmitic acid (4 mCi/mmol) (American Radiolabeled Chemicals) complexed to BSA (palmitic acid:albumin molar ratio of 4:1). After a 7-h incubation, the medium was collected and slices were washed with 2 ml of saline solution and homogenized in Tris buffer (25 mM Tris-HCl, pH 8.0; 50 mM NaCl). Fatty acid uptake ability was calculated as the sum of palmitic acid converted to CO_2 and ketone bodies with that incorporated into total cellular lipids after incubation. For measurement of CO_2 production by the liver slices, the center wells were placed into scintillation vials containing 4 ml of scintillation cocktail, and radioactivity was counted. For measurement of ketone body generation, aliquots of medium (500 μl) and liver homogenates (250 μl) were treated with ice-cold perchloric acid to make final concentrations of 200 mM and were centrifuged at 3,000 *g* for 20 min at 4°C. Aliquots of the supernatant containing the ketone bodies were introduced into the scintillation vials, and radioactivity was counted. Total cellular lipids were extracted from the liver homogenates according to a modified method developed by Folch et al. (53), collected into scintillation vials, and evaporated to dryness under an air stream; radioactivity was then counted. The experiment was repeated 3 times, and palmitic acid uptake ability was expressed as fold changes relative to that of *Ppara*$^{+/+}$ nontransgenic mice.

Other methods. To determine the hepatic content of lipids and lipid peroxides, lipids were extracted according to a method by Folch et al. (53). Triglycerides and free fatty acids were measured with a Triglyceride E-test kit and a NEFA C-test kit (Wako), respectively. Lipid peroxides (malondialdeyde and 4-hydroxyalkenals) were measured using an LPO-586 kit (OXIS International). Hepatic β-oxidation activity was determined as described previously (16). Hepatic caspase 3 activity was measured as described elsewhere (54). Plasma glucose and insulin levels were determined using a Glucose CII-test kit (Wako) and a mouse insulin ELISA kit (U-type, AKRIN-031; Shibayagi), respectively.

Statistics. Statistical analysis was performed with a 2-tailed Student's *t* test for quantitative variables or with a chi-square test for qualitative variables. Quantitative data are expressed as the mean ± SD. $P < 0.05$ was considered to be statistically significant.

Acknowledgments

We thank Trevor Ralph for editorial assistance and Chikako Tanaka for helpful suggestions.

Received for publication August 13, 2007, and accepted in revised form November 7, 2007.

Address correspondence to: Naoki Tanaka, Department of Metabolic Regulation, Institute on Aging and Adaptation, Shinshu University Graduate School of Medicine, Asahi 3-1-1, Matsumoto 390-8621, Japan. Phone: 81-263-37-2850; Fax: 81-263-37-3094; E-mail: naopi@hsp.md.shinshu-u.ac.jp.

1. Kiyosawa, K., et al. 1990. Interrelationship of blood transfusion, non-A, non-B hepatitis and heparocellular carcinoma: analysis by detection of antibody to hepatitis C virus. *Hepatology.* **12**:671–675.
2. Kiyosawa, K., et al. 2004. Hepatocellular carcinoma: recent trends in Japan. *Gastroenterology.* **127**(5 Suppl. 1):S17–S26.
3. Tanaka, Y., et al. 2002. Inaugural article: a comparison of the molecular clock of hepatitis C virus in the United States and Japan predicts that hepatocellular carcinoma incidence in the United States will increase over the next two decades. *Proc. Natl. Acad. Sci. U. S. A.* **99**:15584–15589.
4. Okuda, K., Fujimoto, I., Hanai, A., and Urano, Y. 1987. Changing incidence of heparocellular carcinoma in Japan. *Cancer Res.* **47**:4967–4972.
5. El-Serag, H.B., and Mason, A.C. 1999. Rising incidence of hepatocellular carcinoma in the United States. *N. Engl. J. Med.* **340**:745–750.
6. Shimotohno, K. 2000. Hepatitis C virus and its pathogenesis. *Semin. Cancer Biol.* **10**:233–240.
7. Moriya, K., et al. 1997. Hepatitis C virus core protein induces hepatic steatosis in transgenic mice. *J. Gen. Virol.* **78**:1527–1531.
8. Shintani, Y., et al. 2004. Hepatitis C virus infection and diabetes: direct involvement of the virus in the development of insulin resistance. *Gastroenterology.* **126**:840–848.
9. Moriya, K., et al. 1998. The core protein of hepatitis C virus induces hepatocellular carcinoma in transgenic mice. *Nat. Med.* **4**:1065–1068.
10. Powell, E.E., Jonsson, J.R., and Clouston, A.D. 2005. Steatosis: co-factor in other liver diseases. *Hepatology.* **42**:5–13.
11. Ohata, K., et al. 2003. Hepatic steatosis is a risk factor for heparocellular carcinoma in patients with chronic hepatitis C virus infection. *Cancer.* **97**:3036–3043.
12. Browning, J.D., and Horton, J.D. 2004. Molecular mediators of hepatic steatosis and liver injury. *J. Clin. Invest.* **114**:147–152.
13. Le, T.H., et al. 2004. The zonal distribution of megamitochondria with crystalline inclusions in nonalcoholic steatohepatitis. *Hepatology.* **39**:1423–1429.
14. Yang, S., Lin, H.Z., Hwang, J., Chacko, V.P., and Diehl, A.M. 2001. Hepatic hyperplasia in noncirrhotic fatty livers: is obesity-related hepatic steatosis a premalignant condition? *Cancer Res.* **61**:5016–5023.
15. Desvergne, B., and Wahli, W. 1999. Peroxisome proliferator-activated receptors: nuclear control of metabolism. *Endocr. Rev.* **20**:649–688.
16. Aoyama, T., et al. 1998. Altered constitutive expression of fatty acid-metabolizing enzymes in mice lacking the peroxisome proliferator-activated receptor α (PPARα). *J. Biol. Chem.* **273**:5678–5684.
17. Staels, B., et al. 1998. Mechanism of action of fibrates on lipid and lipoprotein metabolism. *Circulation.* **98**:2088–2093.
18. Harano, Y., et al. 2006. Fenofibrate, a peroxisome proliferator-activated receptor α agonist, reduces hepatic steatosis and lipid peroxidation in fatty liver Shionogi mice with hereditary fatty liver. *Liver Int.* **26**:613–620.
19. Yeldandi, A.V., Rao, M.S., and Reddy, J.K. 2000. Hydrogen peroxide generation in peroxisome proliferator-induced oncogenesis. *Mutat. Res.* **448**:159–177.
20. Yu, S., Rao, M.S., and Reddy, J.K. 2003. Peroxisome proliferator-activated receptors, fatty acid oxidation, steatohepatitis and hepatocarcinogenesis. *Curr. Mol. Med.* **3**:561–572.
21. Peters, J.M., Cattley, R.C., and Gonzalez, F.J. 1997. Role of PPARα in the mechanism of action of the nongenotoxic carcinogen and peroxisome proliferator Wy-14,643. *Carcinogenesis.* **18**:2029–2033.
22. Fan, C.Y., et al. 1998. Steatohepatitis, spontaneous peroxisome proliferation and liver tumors in mice lacking peroxisomal fatty acyl-CoA oxidase. Implications for peroxisome proliferator-activated receptor α natural ligand metabolism. *J. Biol. Chem.* **273**:15639–15645.
23. Moriya, K., et al. 2001. Oxidative stress in the absence of inflammation in a mouse model for hepatitis C virus-associated hepatocarcinogenesis. *Cancer Res.* **61**:4365–4370.
24. Lee, S.S., et al. 1995. Targeted disruption of the α isoform of the peroxisome proliferator-activated receptor gene in mice results in abolishment of the pleiotropic effects of peroxisome proliferators. *Mol. Cell. Biol.* **15**:3012–3022.
25. Mandard, S., Muller, M., and Kersten, S. 2004. Peroxisome proliferator-activated receptor α target genes. *Cell. Mol. Life Sci.* **61**:393–416.
26. Peters, J.M., et al. 1998. Role of peroxisome proliferator-activated receptor α in altered cell cycle regulation in mouse liver. *Carcinogenesis.* **19**:1989–1994.
27. Tsutsumi, T., et al. 2002. Interaction of hepatitis C virus core protein with retinoid X receptor α modulates its transcriptional activity. *Hepatology.* **35**:937–946.
28. Tanaka, N., et al. 2003. In vivo stabilization of nuclear retinoid X receptor α in the presence of peroxisome proliferator-activated receptor α. *FEBS Lett.* **543**:120–124.
29. Moriishi, K., et al. 2007. Critical role of PA28γ in hepatitis C virus-associated steatogenesis and hepatocarcinogenesis. *Proc. Natl. Acad. Sci. U. S. A.* **104**:1661–1666.
30. Perlemuter, G., et al. 2002. Hepatitis C virus core

protein inhibits microsomal triglyceride transfer protein activity and very low density lipoprotein secretion: a model of viral-related steatosis. *FASEB J.* **16**:185–194.
31. Korenaga, M., et al. 2005. Hepatitis C virus core protein inhibits mitochondrial electron transport and increases reactive oxygen species (ROS) production. *J. Biol. Chem.* **280**:37481–37488.
32. Gomez-Gonzalo, M., et al. 2004. Hepatitis C virus core protein regulates p300/CBP co-activation function. Possible role in the regulation of NF-AT1 transcriptional activity. *Virology.* **328**:120–130.
33. Yu, S., and Reddy, J.K. 2007. Transcription coactivators for peroxisome proliferator-activated receptors. *Biochim. Biophys. Acta.* **1771**:936–951.
34. Spaziani, A., Alisi, A., Sanna, D., and Balsano, C. 2006. Role of p38 MAPK and RNA-dependent protein kinase (PKR) in hepatitis C virus core-dependent nuclear delocalization of cyclin B1. *J. Biol. Chem.* **281**:10983–10989.
35. Diradourian, C., Girard, J., and Pegorier, J.P. 2005. Phosphorylation of PPARs: from molecular characterization to physiological relevance. *Biochimie.* **87**:33–38.
36. Reddy, J.K., Rao, M.S., Azarnoff, D.L., and Sell, S. 1979. Mitogenic and carcinogenic effects of a hypolipidemic peroxisome proliferator, [4-chloro-6-(2,3-xylidino)-2- pyrimidinylthio]acetic acid (Wy-14,643), in rat and mouse liver. *Cancer Res.* **39**:152–161.
37. Rao, M.S., and Reddy, J.K. 1996. Hepatocarcinogenesis of peroxisome proliferators. *Ann. N. Y. Acad. Sci.* **804**:573–587.
38. Genini, D., and Catapano, C.V. 2006. Control of peroxisome proliferator-activated receptor fate by the ubiquitin-proteasome system. *J. Recept. Signal. Transduct. Res.* **26**:679–692.
39. Dharancy, S., et al. 2005. Impaired expression of the peroxisome proliferator-activated receptor alpha during hepatitis C virus infection. *Gastroenterology.* **128**:334–342.
40. de Gottardi, A., et al. 2006. Peroxisome proliferator-activated receptor-alpha and -gamma mRNA levels are reduced in chronic hepatitis C with steatosis and genotype 3 infection. *Aliment. Pharmacol. Ther.* **23**:107–114.
41. Lefkowitch, J.H., et al. 1993. Pathological diagnosis of chronic hepatitis C: a multicenter comparative study with chronic hepatitis B. *Gastroenterology.* **104**:595–603.
42. Moriya, K., et al. 2001. Increase in the concentration of carbon 18 monounsaturated fatty acids in the liver with hepatitis C: analysis in transgenic mice and humans. *Biochem. Biophys. Res. Commun.* **281**:1207–1212.
43. Barbaro, G., et al. 1999. Hepatocellular mitochondrial alterations in patients with chronic hepatitis C: ultrastructural and biochemical findings. *Am. J. Gastroenterol.* **94**:2198–2205.
44. Hui, J.M., et al. 2003. Insulin resistance is associated with chronic hepatitis C virus infection and fibrosis progression [corrected]. *Gastroenterology.* **125**:1695–1704.
45. Kato, J., et al. 2001. Normalization of elevated hepatic 8-hydroxy-2'-deoxyguanosine levels in chronic hepatitis C patients by phlebotomy and low iron diet. *Cancer Res.* **61**:8697–8702.
46. Horiike, S., et al. 2005. Accumulation of 8-nitroguanine in the liver of patients with chronic hepatitis C. *J. Hepatol.* **43**:403–410.
47. Takenaka, K., et al. 1994. Possible multicentric occurrence of hepatocellular carcinoma: a clinicopathological study. *Hepatology.* **19**:889–894.
48. Oikawa, T., et al. 2005. Multistep and multicentric development of hepatocellular carcinoma: histological analysis of 980 resected nodules. *J. Hepatol.* **42**:225–229.
49. Akiyama, T.E., et al. 2001. Peroxisome proliferator-activated receptor-α regulates lipid homeostasis, but is not associated with obesity. *J. Biol. Chem.* **276**:39088–39093.
50. Nakajima, T., et al. 2004. Peroxisome proliferator-activated receptor α protects against alcohol-induced liver damage. *Hepatology.* **40**:972–980.
51. Ni, R., et al. 1994. Fas-mediated apoptosis in primary cultured mouse hepatocytes. *Exp. Cell Res.* **215**:332–337.
52. Graulet, B., Gruffat, D., Durand, D., and Bauchart, D. 1998. Fatty acid metabolism and very low density lipoprotein secretion in liver slices from rats and preruminant calves. *J. Biochem.* **124**:1212–1219.
53. Folch, J., Lees, M., and Sloane Stanley, G.H. 1957. A simple method for the isolation and purification of total lipids from animal tissues. *J. Biol. Chem.* **226**:497–509.
54. Gurtu, V., Kain, S.R., and Zhang, G. 1997. Fluorometric and colorimetric detection of caspase activity associated with apoptosis. *Anal. Biochem.* **251**:98–102.

Clinical and Experimental Immunology ORIGINAL ARTICLE doi:10.1111/j.1365-2249.2006.03290.x

Combined therapy of transcatheter hepatic arterial embolization with intratumoral dendritic cell infusion for hepatocellular carcinoma: clinical safety

Y. Nakamoto,* E. Mizukoshi,* H. Tsuji,* Y. Sakai,* M. Kitahara,* K. Arai,* T. Yamashita,* K. Yokoyama,† N. Mukaida,‡ K. Matsushima,§ O. Matsui¶ and S. Kaneko*

*Disease Control and Homeostasis, †Department of Biotracer Medicine, Graduate School of Medical Science, Kanazawa, Japan, ‡Division of Molecular Bioregulation, Cancer Research Institute, Kanazawa University, Kanazawa, Japan, §Department of Molecular Preventive Medicine, Graduate School of Medicine, University of Tokyo, Japan, and ¶Department of Radiology, Graduate School of Medicine, Kanazawa University, Kanazawa, Japan

Accepted for publication 16 November 2006
Correspondence: Shuichi Kaneko MD, PhD, Disease Control and Homeostasis, Graduate School of Medical Science, Kanazawa University, 13–1 Takara-machi, Kanazawa 920–8641, Japan.
E-mail: skaneko@m-kanazawa.jp

Summary

The curative treatments for hepatocellular carcinoma (HCC), including surgical resection and radiofrequency ablation (RFA), do not prevent tumour recurrence effectively. Dendritic cell (DC)-based immunotherapies are believed to contribute to the eradication of the residual and recurrent tumour cells. The current study was designed to assess the safety and bioactivity of DC infusion into tumour tissues following transcatheter hepatic arterial embolization (TAE) for patients with cirrhosis and HCC. Peripheral blood mononuclear cells (PBMCs) were differentiated into phenotypically confirmed DCs. Ten patients were administered autologous DCs through an arterial catheter during TAE treatment. Shortly thereafter, some HCC nodules were treated additionally to achieve the curative local therapeutic effects. There was no clinical or serological evidence of adverse events, including hepatic failure or autoimmune responses in any patients, in addition to those due to TAE. Following the infusion of ^{111}Indium-labelled DCs, DCs were detectable inside and around the HCC nodules for up to 17 days, and were associated with lymphocyte and monocyte infiltration. Interestingly, T lymphocyte responses were induced against peptides derived from the tumour antigens, Her-2/neu, MRP3, hTERT and AFP, 4 weeks after the infusion in some patients. The cumulative survival rates were not significantly changed by this strategy. These results demonstrate that transcatheter arterial DC infusion into tumour tissues following TAE treatment is feasible and safe for patients with cirrhosis and HCC. Furthermore, the antigen-non-specific, immature DC infusion may induce immune responses to unprimed tumour antigens, providing a plausible strategy to enhance tumour immunity.

Keywords: clinical safety, dendritic cells, hepatocellular carcinoma, immunotherapy, transcatheter hepatic arterial embolization

Introduction

Hepatocellular carcinoma (HCC) occurs primarily in individuals with cirrhosis related to either hepatitis C virus (HCV) or hepatitis B virus (HBV) infections [1–3]. The curative treatments for HCC, including surgical resection and percutaneous radiofrequency ablation (RFA), do not prevent tumour recurrence efficiently because active hepatitis and cirrhosis in the surrounding nontumour liver tissues exhibit high carcinogenetic potentials to develop *de novo* HCC [4–7]. In addition, their reduced hepatic reserve due to cirrhosis decreases the tolerance to these local treatments and reduces drug metabolism, including that of anti-cancer agents, and therefore limits their usefulness. Among many novel strategies targeting HCC recurrence, immune-based therapies are believed to enhance the sensitivity, specificity and self-regulation of the immune system to find and eradicate tumour cells wherever they reside [8].

Dendritic cells (DCs) are the most potent type of antigen-presenting cells in the human body, and are involved in the regulation of both innate and adaptive immune responses [9–11]. During DC development, immature DCs exhibit the unique ability to take up and process antigens in the peripheral blood and tissues [12,13]. Subsequently, they migrate to draining lymph nodes, where they must mature to fully activated DCs to present the antigens to resting lymphocytes and elicit T cell responses [14–16]. During the maturation processes, they express high levels of cell-surface major

histocompatibility complex (MHC) antigen complexes and co-stimulatory molecules [17]. So far, most of the DC-based immunotherapies have been performed using intravenous (i.v.), intradermal (i.d.) and subcutaneous (s.c.) routes and lymph node injection following the predictive tumour antigen stimulation *ex vivo* [18,19]. Yet the clinical efficacy remained controversial because consistent tumour destruction or extended life span has not been observed in most treated cancer patients [20–22]. Accordingly, antigen stimulation may not be suitable for cancer treatments, or the proper tumour antigens may not be present to be taken up by DCs after the infusion.

In addition, DCs are reported to induce immune responses to target antigens by a cross-priming mechanism that is greatly enhanced when the target cells are apoptotic [23,24]. Apoptosis of tumour cells is induced by the standard treatments for HCC, i.e. transcatheter hepatic arterial embolization (TAE), percutaneous ethanol injection (PEI), RFA and intra-arterial chemotherapy [25,26]. Importantly, we have observed recently that immune responses specific for tumour antigens and peptides were enhanced during the course of the therapies, while anti-tumour responses were not enough to prevent HCC recurrence [27].

Based on these observations, we suggested a novel DC-based therapy in which immature DCs were injected through an arterial catheter into apoptotic tumour tissues following TAE. Immature DCs were delivered to HCC tumour tissues, by which we hypothesized that the physiological maturation steps including antigen ingestion, migration and presentation might proceed within the patient's body. In the current study, clinical safety was evaluated in patients with HCV-related cirrhosis complicated with HCC. The results suggest that immature DCs were infused successfully and safely to tumour tissues, and immune responses were induced to the tumour antigen peptides with human leucocyte antigen (HLA)-A24 binding motif, which are shared by most Asian individuals.

Patients and methods

Patients

Inclusion criteria were a radiological diagnosis of primary HCC by CT angiography, HCV-related HCC, a Karnofsky score of $\geq$ 70%, an age of $\geq$ 20 years, informed consent, the following normal baseline haematological parameters (within 1 week before DC administration): haemoglobin $\geq$ 8·5 g/dl; white cell count $\geq$ 2000/ml; platelet count $\geq$ 50 000/ml; creatinine < 1·5 mg/dl, and liver damage A or B [28].

Exclusion criteria included severe cardiac, renal, pulmonary, haematological or other systemic disease associated with a discontinuation risk; human immunodeficiency virus (HIV) infection; prior history of other malignancies; history of surgery, chemotherapy or radiation therapy within 4 weeks; immunological disorders including splenectomy and radiation to the spleen; corticosteroid or anti-histamine therapy; current lactation; pregnancy; history of organ transplantation; or difficulty in follow-up.

There were 10 patients enrolled in the study (one woman and nine men), with an age range of 45–79 years (Table 1). Patients with verified radiological diagnoses of HCC stage II or more were eligible and enrolled in this study. Similarly, a group of 11 patients treated with TAE without DC administration was also enrolled in this study as a control. The Institutional Review Board reviewed and approved the study protocol. This study complied with ethical standards outlined in the Declaration of Helsinki. Adverse events were monitored for 1 month after the DC infusion in terms of fever, vomiting, abdominal pain, encephalopathy, myalgia, ascites, gastrointestinal disorder, bleeding, hepatic abscess and autoimmune diseases.

Preparation and injection of autologous DCs

DCs were generated from blood monocyte precursors as reported previously [29,30]. Briefly, peripheral blood mononuclear cells (PBMCs) were isolated by centrifugation in Lymphoprep™ Tubes (Nycomed, Roskilde, Denmark). For generating DCs, PBMCs were plated in six-well tissue culture dishes (Costar, Cambridge, MA, USA) at $1{\cdot}4 \times 10^7$ cells in 2-ml per well and allowed to adhere to plastic for 2 h. Adherent cells were cultured in RPMI-1640 supplemented with 1% heat-inactivated autologous plasma, 100 U/ml penicillin G (GMP grade; Meiji, Tokyo, Japan), 100 μg/ml streptomycin sulphate (GMP grade; Meiji), 1000 U/ml recombinant human interleukin (IL)-4 (GMP grade; Cell Genix, Freiburg, Germany) and 100 ng/ml recombinant human granulocyte macrophage colony-stimulating factor (GM-CSF) (GMP grade; Novartis, Basel, Switzerland) for 7 days. In the selected cases, the cells were pulsed with 10 μg/ml keyhole limpet haemocyanin (KLH) [depyrogenated, lipopolysaccharide (LPS) free; Calbiochem-Novabiochem Corp., San Diego, CA, USA] overnight 1 day before injection. On day 7, the cells were harvested for injection, 5×10^6 cells were reconstituted in 5 ml normal saline containing 1% autologous plasma, mixed with absorbable gelatin sponge (Gelfoam; Pharmacia & Upjohn, Peapack, NJ, USA) and infused through an arterial catheter following Lipiodol (iodized oil) (Lipiodol Ultrafluide, Laboratoire Guerbet, Aulnay-Sous-Bois, France) injection during selective TAE therapy. Release criteria for DCs were viability > 80%, purity > 30%, negative Gram stain and endotoxin polymerase chain reaction (PCR) and negative in process cultures from samples sent 48 h before release. All products met all release criteria, and the DCs had a typical phenotype of $CD14^-$ and $HLA\text{-}DR^+$.

Flow cytometry analysis

The DC preparation was assessed by staining with the following monoclonal antibodies (MoAb) for 30 min on ice:

Table 1. Patient characteristcs and treatments.

Patient no.	Gender	Age (years)	HLA	TNM stages	No. of tumours	Largest tumour (mm)	Child-Pugh	KPS	Post-TAE Rx	Image complete Rx
1	M	45	A2 A11	IVB	Multiple	50	A	100	No	Complete
2	M	60	A26 A33	II	3	15	A	100	RFA	Incomplete
3	F	70	A3 A24	II	2	15	A	100	RFA	Complete
4	M	77	A2 A24	II	3	10	A	100	RFA	Complete
5	M	73	A24	III	Multiple	70	B	80	Chemo	Incomplete
6	M	62	A24 A26	III	Multiple	32	A	100	RFA	Complete
7	M	67	A11 A24	III	Multiple	35	A	100	Chemo	Incomplete
8	M	60	A2 A24	II	2	40	B	100	MCT	Complete
9	M	79	A2 A33	III	5	60	A	100	RFA	Complete
10	M	76	A11 A24	II	1	45	A	100	Ope	Complete
11	M	71	n.d.	II	1	35	B	100	No	Complete
12	M	68	A24	II	4	20	A	100	RFA	Complete
13	F	66	A2 A24	IVA	3	30	A	100	No	Complete
14	F	68	A11 A33	IVA	Multiple	50	B	100	Chemo	Incomplete
15	F	74	n.d.	II	2	20	B	100	RFA	Complete
16	F	67	A2 A24	III	3	25	A	100	RFA	Incomplete
17	F	70	A2 A11	I	1	20	B	100	No	Complete
18	M	59	n.d.	II	3	20	A	100	RFA	Complete
19	M	68	n.d.	III	Multiple	25	B	100	RFA	Complete
20	M	70	A2 A26	II	5	15	B	100	No	Complete
21	M	80	A2 A24	III	3	38	B	100	No	Complete

Chemo: chemotherapy; Child-Pugh: Child-Pugh classification; HCC: hepatocellular carcinoma; KPS: Karnovsky performance scores; n.d.: not determined; Ope: partial hepatectomy; RFS: percutaneous radiofrequency ablation; Rx: treatment; TAE: transcatheter arterial embolization; TNM: tumour-node metastasis.

anti-CD14-allophycocyanin (APC) (MÖP9), anti-HLA-DR-fluorescein isothiocyanate (FITC) (L243), anti-CD11c-APC (S-HCL-3), anti-CD123-phycoerythrin (PE) (9F5) (BD PharMingen, San Diego, CA, USA), anti-CD80-PE (MAB104), anti-CD83-PE (HB15a) and anti-CD86-PE (HA5·2B7) (Beckman Coulter, Fullerton, CA, USA). Cells were analysed on a FACSCalibur™ flow cytometer. Data analysis was performed with CELLQuest™ software (Becton Dickinson, San Jose, CA, USA).

^{111}Indium oxinate labeling and autoradiography

DCs were labelled with ^{111}Indium (In) oxinate at a specific activity of 32·5 μCi/10^6 cells according to the protocols supplied by the manufacturer (Nihon Medi-Physics, Hyogo, Japan). Scintigraphic images of the depot were acquired with a gamma camera 6, 24, 48 h and 7 days after injection. In one case, the treated HCC nodule was accidentally resected surgically 17 days after DC infusion. Autoradiography was conducted and analysed on a BAS 1000 image analyser (Fuji Photo Film, Tokyo, Japan).

Immunohistochemical analysis

The liver tissues were fixed in buffered zinc formalin (Anatech Ltd, Battle Creek, MI, USA), embedded in paraffin, sectioned (at 3 μm), and stained with haematoxylin and eosin. The paraffin sections were deparaffinized, treated in a pressure cooker for 1–40 min, and incubated with mouse anti-human CD1a (MTB1; 1 : 20 diluted), CD4 (1F6; 1 : 20), CD8 (1A5; 1 : 20), CD20 (7D1; 1 : 100), CD56 (CD564; 1 : 50), CD83 (1H4b; 1 : 20) (Novocastra, Newcastle, UK), CD14 (7; 1 : 20) or HLA-DR (LN3; 1 : 100) (LabVision, Fremont, CA, USA) antibody overnight at 4°C. The cells were then visualized using a Vectastain ABC Standard Kit (Vector Laboratories, Burlingame, CA, USA), and the tissue sections were counterstained with haematoxylin before mounting.

Interferon (IFN)-γ enzyme-linked immunospot (ELISPOT) assay

The prevalence of activated, tumour antigen peptide-specific PBMCs was determined by IFN-γ ELISPOT analysis (Mabtech, Nacka, Sweden). Briefly, 96-well mixed cellulose ester membrane-backed plates (MAHA S4510; Millipore, Bedford, MA, USA) were coated with 100 μl of an anti-IFN-γ MoAb 1-D1K (15 μg/ml; Mabtech) overnight at 4°C. Peptides were added directly to the wells at a final concentration of 10 μg/ml. PBMCs were added to the wells at 3×10^5 cells/well. The plates were incubated at 37°C, 5% CO_2 overnight (14–16 h) and then processed as described [31,32]. ELISPOT assays were conducted in duplicate wells. IFN-γ producing cells were counted by direct visualization and are expressed

as mean number of spots per 3×10^5 cells. The number of specific spots was determined by subtracting the number of spots in the absence of antigen. Responses were considered positive if more than 10 specific spots were detected and if the number of spots in the presence of antigen was at least twofold greater than the number of spots in the absence of antigen. The negative controls consisted of incubation of PBMCs with a peptide representing an HLA-A24 restricted epitope derived from HIV envelope protein ($HIVenv_{584}$) [33] and were always < five spots per 3×10^5 cells. The positive controls consisted of 10 ng/ml phorbol 12-myristate 13-acetate (PMA; Sigma, St. Louis, MO, USA) and 500 ng/ml ionomycin (Sigma) or a cytomegalovirus (CMV) pp65-derived peptide ($CMVpp65_{328}$) [34].

HLA-A24 restricted peptide epitopes used in this study, AFP_{403} (KYIQESQAL), AFP_{424} (EYYLQNAFL), AFP_{434} (AYTKKAPQL), AFP_{357} (EYSRRHPQL) [27], $hTERT_{1088}$ (TYVPLLGSL), $hTERT_{845}$ (CYGDMENKL), $hTERT_{167}$ (AYQVCGPPL) (unpublished), $hTERT_{461}$ (VYGFVRACL), $hTERT_{324}$ (VYAETKHFL) [35], Her-2/neu_8 (RWGLLLALL) [36], $MRP3_{765}$ (VYSDADIFL) and $MRP3_{692}$ (AYVPQQAWI) [37], were synthesized at Mimotope (Melbourne, Australia) and Sumitomo Pharmaceuticals (Osaka, Japan). They were identified using mass spectrometry, and their purities were determined to be > 80% by analytical high performance liquid chromatography (HPLC). Regarding the immunological properties of the epitopes in HCC patients, we found that AFP- and hTERT-derived epitopes were recognized by cytotoxic T lymphocytes in 7·9–21·1% and 6·9–12·5% of 38 and 72 patients, respectively [27,38]. On the other hand, immune responses to Her-2/neu- and MRP3-derived epitopes have not been reported; however, overexpression of Her-2/neu protein was reported to be 2·42% in HCC patients [39], and in our unpublished data the immune responses to Her-2/neu-derived epitope were observed in 5·1% HCC patients (tested 38 patients). In addition, expression of MRP3 protein was reported to be 100% in HCC patients [40]. In our unpublished data, the immune responses to MRP3-derived epitope were observed in 20·5–25·6% HCC patients (38 tested patients).

Statistical analysis

Results are expressed as mean ± s.d. Differences between groups were analysed for statistical significance by the Mann–Whittney *U*-test. The estimated probability of tumour recurrence-free survival was determined using the Kaplan–Meier method. The Mantel–Cox log-rank test was used to compare curves between groups. Any *P*-values less than 0·05 were considered statistically significant.

Results

Isolation and characterization of DCs

Adherent cells isolated from PBMCs were differentiated into DCs in the presence of IL-4 and granulocyte–macrophage colony-stimulating factor (GM-CSF). DCs from each study patient were shown to develop high levels of MHC class II (HLA-DR) and co-stimulatory molecule B7-2 (CD86) and showed the absence of markers for mature monocytes (CD14). In addition, DCs obtained were phenotypically immature ($CD80^{low}CD83^{low}$) and classified to myeloid ($CD11c^+CD123^-$) and plasmacytoid ($CD11c^-CD123^+$) subsets (Table 2). Furthermore, sufficient numbers (at least 1×10^7) of functional DCs were isolated from 200 ml of peripheral blood in all patients in this clinical trial.

Safety of autologous DC administration

DC administration was performed during TAE therapy, in which DCs were mixed together with Gelfoam and infused through an arterial catheter following Lipiodol injection. Adverse events were monitored clinically and biochemically after DC infusion (Table 3). There were no grades III or IV National Cancer Institute common toxicity criteria adverse

Table 2. Properties of infused dendritic cells.

		lin⁻ HLA-DR⁺				
Patient no.	%$CD14^-$ HLA-DR^+	%$CD11c^+$ $CD123^-$	%$CD11c^-$ $CD123^+$	%$CD80^+$	%$CD83^+$	%$CD86^+$
1	34·5	5·8	8·4	1·6	1·9	11·5
2	56·2	49·7	39·3	4·1	3·2	92·4
3	35·6	63·6	6·1	0	5·7	96·0
4	32·7	22·6	56·5	1·9	1·2	61·6
5	40·4	24·3	57·3	34·9	27·7	94·4
6	60·4	35·8	47·0	11·4	1·5	84·4
7	46·4	54·7	10·7	12·9	12·5	83·2
8	62·8	7·6	32·3	19·0	20·5	49·1
9	55·2	35·2	35·5	28·8	18·3	73·0
10	34·0	9·5	7·0	12·1	8·4	31·8
Mean	45·8	30·9	30·0	12·7	10·1	67·7
s.d.	11·9	20·5	20·5	11·9	9·3	28·9

Table 3. General clinical outcome.

Patient no.	Adverse events: Fever (days)	Vomiting	Abdominal pain	Encephalopathy	Others	DTH to KLH	Tumour recurrence	Survival w/o HCC (months)	Survival (months)	Death/alive
1	1	No	No	No	No	n.d.	Yes	6	17	Death
2	2	No	No	No	No	n.d.	Yes	13	17	Alive
3	No	No	No	No	No	n.d.	Yes	8	30	Alive
4	4	Yes	No	No	No	n.d.	Yes	11	36	Alive
5	No	No	No	No	No	n.d.	n.d.	2	2	Death
6	No	No	No	No	No	n.d.	Yes	5	34	Alive
7	8	No	No	No	No	n.d.	Yes	14	22	Death
8	No	No	No	No	No	Positive	No	9	9	Death
9	5	Yes	No	No	No	n.d.	Yes	6	30	Alive
10	No	No	No	No	No	Positive	Yes	22	24	Alive
Mean								9·6	22·1	
s.d.								5·7	11·0	
11	No	No	No	No	No	n.d.	Yes	4	6	Death
12	No	No	No	No	No	n.d.	Yes	9	24	Death
13	No	No	Yes	No	No	n.d.	Yes	2	8	Alive
14	No	Yes	Yes	No	No	n.d.	Yes	3	9	Death
15	3	No	No	No	No	n.d.	Yes	18	20	Death
16	1	No	No	No	No	n.d.	Yes	8	36	Alive
17	No	No	No	No	No	n.d.	Yes	6	12	Death
18	No	No	No	No	No	n.d.	Yes	11	36	Alive
19	5	No	Yes	Yes	No	n.d.	Yes	7	30	Alive
20	No	No	No	No	No	n.d.	Yes	5	11	Death
21	No	No	No	No	No	n.d..	n.d.	4	4	Alive
Mean								7·0	17·8	
s.d.								4·5	12·0	

Adverse events/others: myalgia, gastrointestinal disorder, bleeding, hepatic abcess and autoimmune diseases; DTH: delayed-type hypersensitivity skin test; KLH: keyhole limpet haemocyanin; n.d.: not determined.

events associated with DC infusion and TAE in this study. Furthermore, the adverse events of the patients treated with DC infusion and TAE were compared with the control patients treated with TAE alone in terms of fever, vomiting, abdominal pain, encephalopathy, myalgia, ascites, gastrointestinal disorders, bleeding, hepatic abscess and autoimmune diseases. Although the clinical courses of five of the patients infused with DCs were complicated with high fever, there were no significant differences in the frequency or severity of adverse events associated with DC infusion. There was also no clinical or serological evidence of hepatic failure or autoimmune response in any patients. Thus, the current treatment of DC infusion was performed safely at the same time as TAE in patients with cirrhosis and HCC.

Kinetics and *in situ* effects of DCs following infusion into HCC tissues

DCs were labelled with ^{111}In-oxine and infused into tumour tissues through an arterial catheter following TAE in two patients (numbers 9 and 10). The kinetics of ^{111}In-labelled DCs were monitored by a gamma camera after the infusion (Fig. 1a). Radioactivity at the tumour site decreased after the infusion, but was still detectable up to 14 days after the infusion, indicating that the DCs stayed alive for more than 2 weeks. However, tracking of labelled DCs to regional lymph nodes was not seen in the current imaging, due possibly to insufficient numbers of migrated DCs, or otherwise due to DC paralysis in tumour tissues [41].

One of the patients (number 10) proceeded unexpectedly to curative surgery 17 days after the DC infusion. The tissue radioactivity was investigated using autoradiography and analysed on an image analyser (Fig. 1b,c,d). Surprisingly, radioactivity was still detectable in the tumour tissue and surrounding liver parenchyma. In addition, immunohistochemistry of the liver tissue was performed using MoAbs specific for cell surface markers CD8, CD14 (monocyte), CD20 (B cell), CD1a (DC) HLA-DR (antigen-presenting cell) and CD83 (DC maturation/activation) (Fig. 2). Immunohistochemical analysis revealed many CD1a-positive DCs in the area surrounding HCC nodules treated with autologous DCs and TAE 17 days previously. In addition, CD83-positive cells and HLA-DR-positive antigen-presenting cells were seen in the same areas of liver tissue. Interestingly, CD83-positive cells were rarely detected in liver tissues of HCC patients, as reported previously [42]. Many $CD8^+$ T cells, $CD14^+$ monocytes and $CD20^+$ B cells were recruited in the same area. In conjunction with the detection of

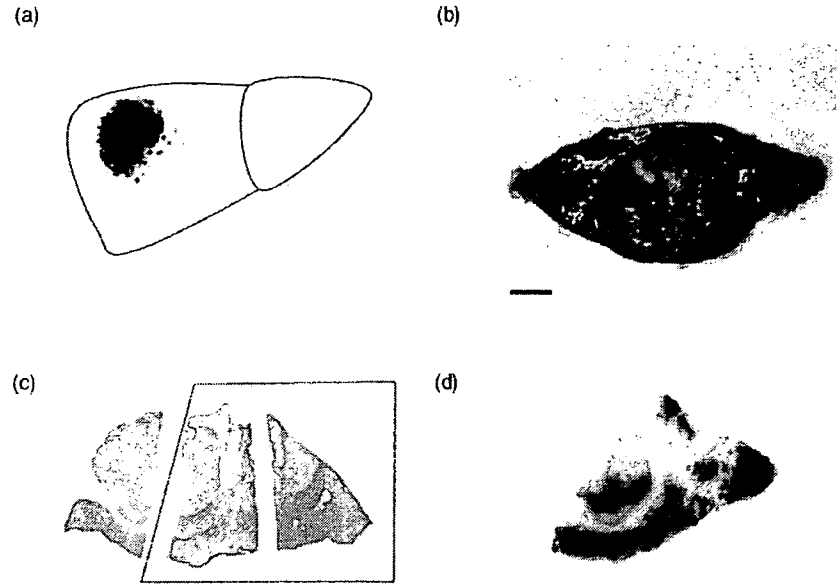

Fig. 1. Kinetics of autologous dendritic cells (DCs) following infusion into tumour tissues in patients with hepatocellular carcinoma (HCC). DCs were labelled with ^{111}In-oxine and infused into tumour tissues through an arterial catheter following transcatheter hepatic arterial embolization (TAE). (a) Scintigraphic images of the depot were acquired with a gamma camera 7 days after injection. (b) In one case, the treated HCC nodule was accidentally resected surgically 17 days after DC infusion. Bar represents 1 cm. Resected tissues were stained with haematoxylin and eosin (c) and, using the tissue comparable to the inset in (c), autoradiography was conducted and analysed on an image analyser (d).

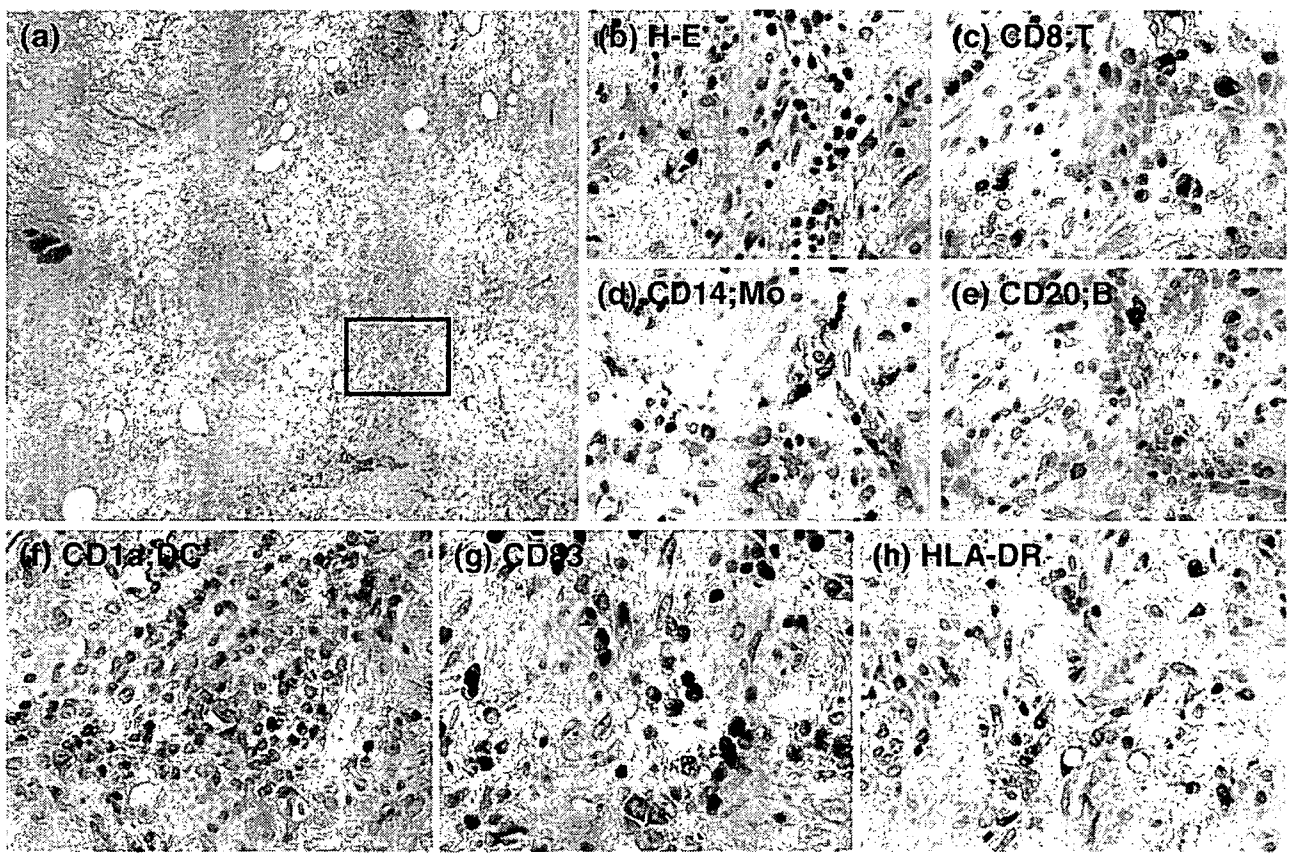

Fig. 2. Immunohistochemical analysis of a surgically resected liver tissue containing a nodule of hepatocellular carcinoma in a patient infused with autologous dendritic cells (DCs) 17 days previously, described in the legend to Fig. 1. The liver tissue was stained with haematoxylin and eosin (a and b) and for CD8 (c), CD14 (d), CD20 (e), CD1a (f), CD83 (g) and human leucocyte antigen D-related (HLA-DR) (h). (b) Close-up of the inset in (a). Areas comparable to (b) are indicated in (c–h). Cells were stained positively in brown. Original magnifications, ×40 (a) and ×400 (b–h).

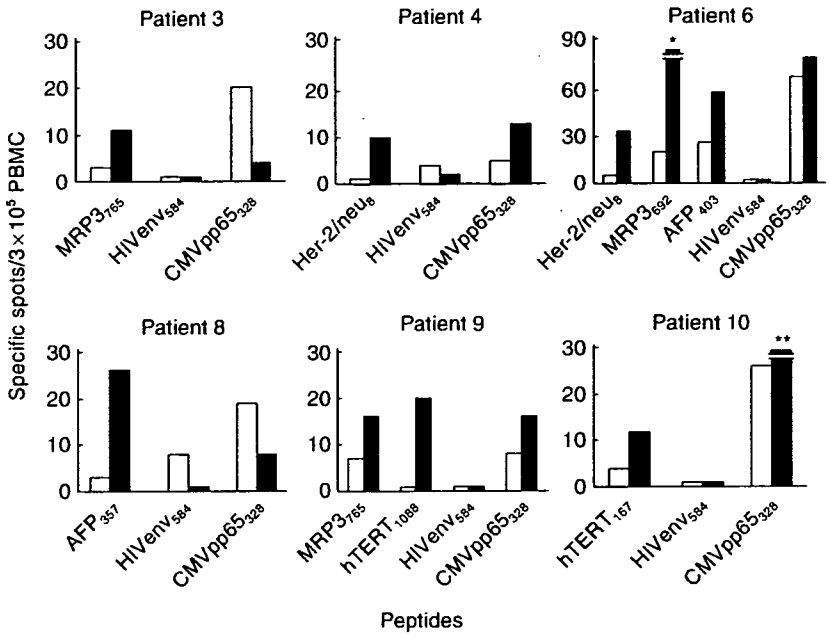

Fig. 3. Immune responses to human leucocyte antigen (HLA)-A24 restricted peptide epitopes derived from tumour antigens in patients infused with dendritic cells (DCs). Peripheral blood mononuclear cells (PBMCs) were obtained before (open bars) and 4 weeks after the infusion (solid bars), pulsed with the peptides derived from AFP, hTERT, Her-2/neu and MRP3, and interferon (IFN)-ã production was quantified by enzyme-linked immunospot assay (ELISPOT). Negative controls consisted of incubation of PBMC with a peptide representing an HLA-A24 restricted epitope derived from HIV envelope protein ($HIVenv_{584}$). Positive controls consisted of 10 ng/ml phorbol 12-myristate 13-acetate (PMA) and 500 ng/ml ionomycin or a cytomegalovirus (CMV) pp65-derived peptide ($CMVpp65_{328}$). Responses were considered positive if more than 10 specific spots were detected and if the number of spots in the presence of peptide was at lease twofold greater than the number of spots in the absence of peptide. *230 specific spots; **32 specific spots.

radioactivity, these data indicate that DCs were viable for more than 17 days following the infusion and seemed to contribute to the recruitment and activation of immune cells.

Immune responses induced following DC infusion

To evaluate the immunomodulatory effects of DCs infused into HCC tissues, PBMCs were obtained 4 weeks after the infusion, pulsed with the peptides derived from AFP, hTERT, Her-2/neu and MRP3 and IFN-ã production was quantified by ELISPOT. Interestingly, frequencies of IFN-ã-producing cells in response to stimulation with HLA-A24-restricted peptide epitopes derived from tumour antigens, Her-2/neu, MRP3, hTERT and AFP, were increased 2–20-fold in six of the eight HLA-A24-positive patients after the treatments (Fig. 3). In addition, in two of the cases DCs were stimulated with KLH before the infusion, and the intradermal test was performed 2 weeks later. Both cases displayed a positive reaction (Table 3), indicating that DCs induced cellular immunity successfully following the treatments [43]. Collectively, these results demonstrated that DC infusion induced immune responses to unprimed tumour antigens, suggesting that antigen-non-specific immature DCs in the tumour tissues enhanced tumour immunity *in vivo*.

Recurrence-free survival following DC infusion

A further objective of this study was to determine the clinical response to DC infusion. Therefore, we compared recurrence-free survival between patients treated with TAE with ($n = 10$) and without ($n = 11$) DC administration (Table 3). While there was a trend for the patients infused with DCs to display longer recurrence-free survival, these differences did not reach statistical significance [mean recurrence-free survival (± s.d.) of patients with and without DC administration: 9·6 ± 5·7 and 7·0 ± 4·5 months, respectively; $P = 0{\cdot}13$]. In addition, there was no correlation between infused DC phenotypes characterized by the surface markers (Table 2) and recurrence-free survival after the infusion. Although the strong $CD8^+$ response against $MRP3_{692}$ was induced in patient 6 (Fig. 3) the clinical outcomes, including recurrence-free survival, were not distinct from the other DC-treated patients.

Discussion

Tumour recurrence rates after curative treatments for HCC are extremely high in patients with active hepatitis and cirrhosis related to HBV and HCV infections [4–6]. Although current treatments, including surgical resection and RFA,

displayed almost complete prevention of local recurrence in the cirrhotic liver, the surrounding non-tumour liver tissues exhibited high carcinogenetic potentials to develop *de novo* HCC. Significant risk factors for recurrence have been reported to be cirrhosis and a higher grade of hepatitis activity [44–46]. IFN therapy and anti-inflammatory drugs have been implicated in the reduction of HCC recurrence [47,48]; however, they did not prevent recurrence satisfactorily. To develop novel therapies targeting HCC recurrence, many immune-based trials have been performed [8].

The current study indicates that immature DC infusion following TAE therapy did not cause additional adverse events in patients with cirrhosis and HCC, and that infused DCs remained alive around the tumour tissues for more than 17 days, as indicated by monitoring the kinetics of ^{111}In-DC, and contributed to the recruitment and activation of immune cells *in situ*. Immune responses were induced to the tumour antigen peptides with HLA-A24 binding motif. Furthermore, intradermal tests were positive when stimulated with KLH. Ultimately, the patients treated with this DC-based immunotherapy did not display statistically longer recurrence-free survival. This study demonstrated the feasibility, safety and bioactivity of transcatheter arterial DC infusion into tumour tissues for patients with cirrhosis and HCC. The data suggest the ability of an active immunotherapeutic strategy to generate antigen-specific cytotoxicity in HCC patients.

Transcatheter arterial DC infusion into tumour tissues following TAE treatment was feasible and safe for patients with cirrhosis and HCC whose hepatic reserve was decreased, similar to reports from other DC immunotherapy trials [20–22]. Mild toxicity included more patients with fever compared to TAE treatment alone, while their durations were comparable. Two patients complained of infrequent vomiting. To date, no clinical or radiological features of autoimmune diseases have been detected in the current study, nor have other DC immunotherapy trials reported any significant autoimmune events [20–22].

^{111}In-labelled DCs were detectable inside and around the HCC nodules after the infusion, suggesting that they were infused precisely to the targeted nodules and stayed alive longer than expected. If DCs died after the infusion, the radioactive materials should have been released from the labelled DCs. Furthermore, they seemed to contribute to the recruitment and activation of immune cells by immunohistochemical analysis. In this procedure, immature DCs that did not express CD83 molecule were infused to liver tissues, and only a few infiltrating inflammatory cells were reported to express CD83 in liver tissues [42,49]. However, many immune cells were shown to express CD83 in the tissues surrounding the treated HCC nodules. As CD83 expression is known to be limited on mature DCs and activated B lymphocytes [50,51], the infused immature DCs were suggested to become mature after the infusion, and to recruit activated lymphocytes in the liver tissues.

Interestingly, the results demonstrate that the antigen-non-specific, immature DC infusion may induce the immune responses to unprimed tumour antigens. Because immature DCs are known to display high endocytic and phagocytic activity [52,53], they can take up tumour antigens in the apoptotic tissues treated with TAE therapy. Following the endocytosis and phagocytosis of tumour antigens, DCs may move to secondary lymphoid organs, including regional lymph nodes, become activated and mature and induce antigen-specific cell-mediated and humoral immune responses. Even uncharacterized antigens can be processed and presented to the host immune systems by DCs in this study, and the immune responses to unprimed antigens may be induced. The current *in vivo* immune induction may omit the identification of tumour antigenic epitopes from the development of tumour immunotherapy.

The recurrence-free survival rates were not increased significantly by this strategy. This therapeutic effect was probably limited due to the insufficient anti-tumour immune responses. To enhance the tumour antigen presentation to T lymphocytes, DCs could be transduced with MHC class I and class II genes [54,55] and co-stimulatory molecules, e.g. CD40, CD80 and CD86 [56,57], and loaded with tumour-associated antigens including tumour lysates, peptides and RNA transfection [58]. To induced natural killer (NK) and NK T cell activation, DCs could be stimulated and modified to produce larger amounts of cytokines, e.g. IL-12, IL-18 and type I IFN [57,59]. Furthermore, DC migration in secondary lymphoid organs could be induced by expression and transduction of chemokine genes, e.g. CCR7 [60–62], by maturation using inflammatory cytokines [63], matrix metalloproteinases and Toll-like receptor (TLR) ligands [64], and by combination of different administration routes including i.v. and i.d. injections [65]. Importantly, the current study suggests an initial strategy to develop a novel immunotherapy with DCs for the prevention of HCC recurrence.

Acknowledgements

We thank Akemi Nakano, Chiharu Minami, Yuzu Hasebe and Hitomi Fuke for technical assistance.

References

1 Tsukuma H, Hiyama T, Tanaka S *et al.* Risk factors for hepatocellular carcinoma among patients with chronic liver disease. N Engl J Med 1993; **328**:1797–801.

2 Velazquez RF, Rodriguez M, Navascues CA *et al.* Prospective analysis of risk factors for hepatocellular carcinoma in patients with liver cirrhosis. Hepatology 2003; 37:520–7.

3 Sangiovanni A, Del Ninno E, Fasani P *et al.* Increased survival of cirrhotic patients with a hepatocellular carcinoma detected during surveillance. Gastroenterology 2004; 126:1005–14.

4 Ercolani G, Grazi GL, Ravaioli M *et al.* Liver resection for hepatocellular carcinoma on cirrhosis: univariate and multivariate analysis of risk factors for intrahepatic recurrence. Ann Surg 2003; **237**:536–43.

5 Poon RT, Fan ST, Ng IO, Lo CM, Liu CL, Wong J. Different risk factors and prognosis for early and late intrahepatic recurrence after resection of hepatocellular carcinoma. Cancer 2000; **89**:500–7.

6 Omata M, Tateishi R, Yoshida H, Shiina S. Treatment of hepatocellular carcinoma by percutaneous tumor ablation methods: ethanol injection therapy and radiofrequency ablation. Gastroenterology 2004; **127**:S159–66.

7 Nakamoto Y, Guidotti LG, Kuhlen CV, Fowler P, Chisari FV. Immune pathogenesis of hepatocellular carcinoma. J Exp Med 1998; **188**:341–50.

8 Butterfield LH. Immunotherapeutic strategies for hepatocellular carcinoma. Gastroenterology 2004; **127**:S232–41.

9 Palucka K, Banchereau J. Dendritic cells: a link between innate and adaptive immunity. J Clin Immunol 1999; **19**:12–25.

10 Banchereau J, Briere F, Caux C *et al.* Immunobiology of dendritic cells. Annu Rev Immunol 2000; **18**:767–811.

11 Pulendran B, Banchereau J, Maraskovsky E, Maliszewski C. Modulating the immune response with dendritic cells and their growth factors. Trends Immunol 2001; **22**:41–7.

12 Villadangos JA, Schnorrer P, Wilson NS. Control of MHC class II antigen presentation in dendritic cells: a balance between creative and destructive forces. Immunol Rev 2005; **207**:191–205.

13 Gregoire M, Ligeza-Poisson C, Juge-Morineau N, Spisek R. Anticancer therapy using dendritic cells and apoptotic tumour cells: pre-clinical data in human mesothelioma and acute myeloid leukaemia. Vaccine 2003; **21**:791–4.

14 Sanchez-Sanchez N, Riol-Blanco L, Rodriguez-Fernandez JL. The multiple personalities of the chemokine receptor CCR7 in dendritic cells. J Immunol 2006; **176**:5153–9.

15 Bayry J, Lacroix-Desmazes S, Kazatchkine MD, Hermine O, Tough DF, Kaveri SV. Modulation of dendritic cell maturation and function by B lymphocytes. J Immunol 2005; **175**:15–20.

16 Crittenden MR, Thanarajasingam U, Vile RG, Gough MJ. Intratumoral immunotherapy: using the tumour against itself. Immunology 2005; **114**:11–22.

17 Figdor CG, de Vries IJ, Lesterhuis WJ, Melief CJ. Dendritic cell immunotherapy: mapping the way. Nat Med 2004; **10**:475–80.

18 McIlroy D, Gregoire M. Optimizing dendritic cell-based anticancer immunotherapy: maturation state does have clinical impact. Cancer Immunol Immunother 2003; **52**:583–91.

19 Ribas A, Butterfield LH, Glaspy JA, Economou JS. Current developments in cancer vaccines and cellular immunotherapy. J Clin Oncol 2003; **21**:2415–32.

20 Hsu FJ, Benike C, Fagnoni F *et al.* Vaccination of patients with B-cell lymphoma using autologous antigen-pulsed dendritic cells. Nat Med 1996; **2**:52–8.

21 Nestle FO, Alijagic S, Gilliet M *et al.* Vaccination of melanoma patients with peptide- or tumor lysate-pulsed dendritic cells. Nat Med 1998; **4**:328–32.

22 Tjoa BA, Simmons SJ, Elgamal A *et al.* Follow-up evaluation of a phase II prostate cancer vaccine trial. Prostate 1999; **40**:125–9.

23 Albert ML, Sauter B, Bhardwaj N. Dendritic cells acquire antigen from apoptotic cells and induce class I-restricted CTLs. Nature 1998; **392**:86–9.

24 Albert ML, Pearce SF, Francisco LM *et al.* Immature dendritic cells phagocytose apoptotic cells via alphavbeta5 and CD36, and cross-present antigens to cytotoxic T lymphocytes. J Exp Med 1998; **188**:1359–68.

25 Rai R, Richardson C, Flecknell P, Robertson H, Burt A, Manas DM. Study of apoptosis and heat shock protein (HSP) expression in hepatocytes following radiofrequency ablation (RFA). J Surg Res 2005; **129**:147–51.

26 Kobayashi N, Ishii M, Ueno Y *et al.* Co-expression of Bcl-2 protein and vascular endothelial growth factor in hepatocellular carcinomas treated by chemoembolization. Liver 1999; **19**:25–31.

27 Mizukoshi E, Nakamoto Y, Tsuji H, Yamashita T, Kaneko S. Identification of alpha-fetoprotein-derived peptides recognized by cytotoxic T lymphocytes in HLA-A24+ patients with hepatocellular carcinoma. Int J Cancer 2006; **118**:1194–204.

28 Makuuchi M. General rules for the clinical and pathological study of primary liver cancer, 2nd English edn. Tokyo: Kanehara Ltd, 2003.

29 Reddy A, Sapp M, Feldman M, Subklewe M, Bhardwaj N. A monocyte conditioned medium is more effective than defined cytokines in mediating the terminal maturation of human dendritic cells. Blood 1997; **90**:3640–6.

30 Dhodapkar MV, Steinman RM, Sapp M *et al.* Rapid generation of broad T-cell immunity in humans after a single injection of mature dendritic cells. J Clin Invest 1999; **104**:173–80.

31 Altfeld MA, Trocha A, Eldridge RL *et al.* Identification of dominant optimal HLA-B60- and HLA-B61-restricted cytotoxic T-lymphocyte (CTL) epitopes: rapid characterization of CTL responses by enzyme-linked immunospot assay. J Virol 2000; **74**:8541–9.

32 Goulder PJ, Brander C, Annamalai K *et al.* Differential narrow focusing of immunodominant human immunodeficiency virus gag-specific cytotoxic T-lymphocyte responses in infected African and caucasoid adults and children. J Virol 2000; **74**:5679–90.

33 Ikeda-Moore Y, Tomiyama H, Miwa K *et al.* Identification and characterization of multiple HLA-A24-restricted HIV-1 CTL epitopes. strong epitopes are derived from V regions of HIV-1. J Immunol 1997; **159**:6242–52.

34 Kuzushima K, Hayashi N, Kimura H, Tsurumi T. Efficient identification of HLA-A*2402-restricted cytomegalovirus-specific CD8(+) T-cell epitopes by a computer algorithm and an enzyme-linked immunospot assay. Blood 2001; **98**:1872–81.

35 Arai J, Yasukawa M, Ohminami H, Kakimoto M, Hasegawa A, Fujita S. Identification of human telomerase reverse transcriptase-derived peptides that induce HLA-A24-restricted antileukemia cytotoxic T lymphocytes. Blood 2001; **97**:2903–7.

36 Tanaka H, Tsunoda T, Nukaya I *et al.* Mapping the HLA-A24-restricted T-cell epitope peptide from a tumour-associated antigen HER2/neu: possible immunotherapy for colorectal carcinomas. Br J Cancer 2001; **84**:94–9.

37 Yamada A, Kawano K, Koga M, Matsumoto T, Itoh K. Multidrug resistance-associated protein 3 is a tumor rejection antigen recognized by HLA-A2402-restricted cytotoxic T lymphocytes. Cancer Res 2001; **61**:6459–66.

38 Mizukoshi E, Nakamoto Y, Marukawa Y *et al.* Cytotoxic T cell responses to human telomerase reverse transcriptase in patients with hepatocellular carcinoma. Hepatology 2006; **43**:1284–94.

39 Xian ZH, Zhang SH, Cong WM, Wu WQ, Wu MC. Overexpression/amplification of HER-2/neu is uncommon in hepatocellular carcinoma. J Clin Pathol 2005; **58**:500–3.

40 Nies AT, Konig J, Pfannschmidt M, Klar E, Hofmann WJ, Keppler D. Expression of the multidrug resistance proteins MRP2 and

MRP3 in human hepatocellular carcinoma. Int J Cancer 2001; **94**:492–9.

41 Vicari AP, Chiodoni C, Vaure C *et al.* Reversal of tumor-induced dendritic cell paralysis by CpG immunostimulatory oligonucleotide and anti-interleukin 10 receptor antibody. J Exp Med 2002; **196**:541–9.

42 Chen S, Akbar SM, Tanimoto K *et al.* Absence of CD83-positive mature and activated dendritic cells at cancer nodules from patients with hepatocellular carcinoma: relevance to hepatocarcinogenesis. Cancer Lett 2000; **148**:49–57.

43 Dhodapkar MV, Steinman RM, Krasovsky J, Munz C, Bhardwaj N. Antigen-specific inhibition of effector T cell function in humans after injection of immature dendritic cells. J Exp Med 2001; **193**:233–8.

44 Adachi E, Maeda T, Matsumata T *et al.* Risk factors for intrahepatic recurrence in human small hepatocellular carcinoma. Gastroenterology 1995; **108**:768–75.

45 Tarao K, Takemiya S, Tamai S *et al.* Relationship between the recurrence of hepatocellular carcinoma (HCC) and serum alanine aminotransferase levels in hepatectomized patients with hepatitis C virus-associated cirrhosis and HCC. Cancer 1997; **79**:688–94.

46 Imamura H, Matsuyama Y, Tanaka E *et al.* Risk factors contributing to early and late phase intrahepatic recurrence of hepatocellular carcinoma after hepatectomy. J Hepatol 2003; **38**:200–7.

47 Shiratori Y, Shiina S, Teratani T *et al.* Interferon therapy after tumor ablation improves prognosis in patients with hepatocellular carcinoma associated with hepatitis C virus. Ann Intern Med 2003; **138**:299–306.

48 Mahmood S, Niiyama G, Kawanaka M *et al.* Long term follow-up of a group of chronic hepatitis C patients treated with anti-inflammatory drugs following initial interferon therapy. Hepatol Res 2002; **24**:213.

49 Tanimoto K, Akbar SM, Michitaka K, Horiike N, Onji M. Antigen-presenting cells at the liver tissue in patients with chronic viral liver diseases: CD83-positive mature dendritic cells at the vicinity of focal and confluent necrosis. Hepatol Res 2001; **21**:117–25.

50 Zhou LJ, Schwarting R, Smith HM, Tedder TF. A novel cell-surface molecule expressed by human interdigitating reticulum cells, Langerhans cells, and activated lymphocytes is a new member of the Ig superfamily. J Immunol 1992; **149**:735–42.

51 Hart DN. Dendritic cells: unique leukocyte populations which control the primary immune response. Blood 1997; **90**:3245–87.

52 Cyster JG. Chemokines, sphingosine-1-phosphate, and cell migration in secondary lymphoid organs. Annu Rev Immunol 2005; **23**:127–59.

53 Trombetta ES, Mellman I. Cell biology of antigen processing in vitro and in vivo. Annu Rev Immunol 2005; **23**:975–1028.

54 Lemos MP, Fan L, Lo D, Laufer TM. CD8alpha+ and CD11b+ dendritic cell-restricted MHC class II controls Th1 CD4+ T cell immunity. J Immunol 2003; **171**:5077–84.

55 Lemos MP, Esquivel F, Scott P, Laufer TM. MHC class II expression restricted to CD8alpha+ and CD11b+ dendritic cells is sufficient for control of *Leishmania major*. J Exp Med 2004; **199**:725–30.

56 Ni K, O'Neill HC. The role of dendritic cells in T cell activation. Immunol Cell Biol 1997; **75**:223–30.

57 Andrews DM, Andoniou CE, Scalzo AA *et al.* Cross-talk between dendritic cells and natural killer cells in viral infection. Mol Immunol 2005; **42**:547–55.

58 Heiser A, Coleman D, Dannull J *et al.* Autologous dendritic cells transfected with prostate-specific antigen RNA stimulate CTL responses against metastatic prostate tumors. J Clin Invest 2002; **109**:409–17.

59 Banchereau J, Steinman RM. Dendritic cells and the control of immunity. Nature 1998; **392**:245–52.

60 Forster R, Schubel A, Breitfeld D *et al.* CCR7 coordinates the primary immune response by establishing functional microenvironments in secondary lymphoid organs. Cell 1999; **99**:23–33.

61 Dieu-Nosjean MC, Vicari A, Lebecque S, Caux C. Regulation of dendritic cell trafficking: a process that involves the participation of selective chemokines. J Leukoc Biol 1999; **66**:252–62.

62 Sallusto F, Lanzavecchia A. Understanding dendritic cell and T-lymphocyte traffic through the analysis of chemokine receptor expression. Immunol Rev 2000; **177**:134–40.

63 MartIn-Fontecha A, Sebastiani S, Hopken UE *et al.* Regulation of dendritic cell migration to the draining lymph node: impact on T lymphocyte traffic and priming. J Exp Med 2003; **198**:615–21.

64 Ratzinger G, Stoitzner P, Ebner S *et al.* Matrix metalloproteinases 9 and 2 are necessary for the migration of Langerhans cells and dermal dendritic cells from human and murine skin. J Immunol 2002; **168**:4361–71.

65 Mullins DW, Sheasley SL, Ream RM, Bullock TN, Fu YX, Engelhard VH. Route of immunization with peptide-pulsed dendritic cells controls the distribution of memory and effector T cells in lymphoid tissues and determines the pattern of regional tumor control. J Exp Med 2003; **198**:1023–34.

Prolonged, NK Cell-Mediated Antitumor Effects of Suicide Gene Therapy Combined with Monocyte Chemoattractant Protein-1 against Hepatocellular Carcinoma

Tomoya Tsuchiyama,* Yasunari Nakamoto,* Yoshio Sakai,* Yohei Marukawa,* Masaaki Kitahara,* Naofumi Mukaida,† and Shuichi Kaneko[1]*

Tumor recurrence rates remain high after curative treatments for hepatocellular carcinoma (HCC). Immunomodulatory agents, including chemokines, are believed to enhance the antitumor effects of tumor cell apoptosis induced by suicide gene therapy. We therefore evaluated the immunomodulatory effects of a bicistronic recombinant adenovirus vector (rAd) expressing both HSV thymidine kinase and MCP-1 on HCC cells. Using an athymic nude mouse model (BALB/c-*nu/nu*), primary s.c. tumors (HuH7; human HCC cells) were completely eradicated by rAd followed by treatment with ganciclovir. The same animals were subsequently rechallenged with HCC cells, tumor development was monitored, and the recruitment or activation of NK cells was analyzed immunohistochemically or by measuring IFN-γ mRNA expression. Tumor growth was markedly suppressed as compared with that in mice treated with a rAd expressing the HSV thymidine kinase gene alone ($p < 0.001$). Suppression of tumor growth was associated with the elevation of serum IL-12 and IL-18. During suppression, NK cells were recruited exclusively, and Th1 cytokine gene expression was enhanced in tumor tissues. The antitumor activity, however, was abolished either when the NK cells were inactivated with anti-asialo GM1 Ab or when anti-IL-12 and anti-IL-18 Abs were administered. These results indicate that suicide gene therapy, together with delivery of MCP-1, eradicates HCC cells and exerts prolonged NK cell-mediated antitumor effects in a model of HCC, suggesting a plausible strategy to prevent tumor recurrence. *The Journal of Immunology,* **2007, 178: 574–583.**

Despite curative treatments including surgical resection and liver transplantation for hepatocellular carcinoma (HCC),[2] tumor recurrence rates remain high, probably because of insufficient therapeutic effects and the multicentric development of HCC in cirrhotic liver (1–3). Although nonsurgical treatments of HCC such as radiofrequency ablation, transcatheter arterial embolizations, and transcatheter arterial chemotherapy induce apoptosis of HCC cells, these treatments do not enhance antitumoral immunity sufficiently. Therefore, gene therapy aimed at enhancing antitumor immune responses may be a promising approach to induce sufficient inhibitory effects for the prevention of tumor recurrence.

Although killing tumor cells with cytotoxic genes such as suicide gene/prodrug systems consisting of HSV thymidine kinase (HSV-tk) and ganciclovir (GCV) may lead to the generation of effective immunity (4, 5), cell killing alone is insufficient to increase many antitumor responses (6–8). Recently, however, coexpression of HSV-tk and chemokines was found to increase tumor immunity in animal models in which neither HSV-tk nor chemokine expression alone was sufficient (9). In addition, we previously demonstrated that, at the local treatment site, the antitumor effects of the HSV-tk/GCV system were enhanced by codelivery of MCP-1, a member of the CC chemokine family (8, 10). MCP-1 has been shown to stimulate the cytotoxic activity of monocytes, enhance the expression of adhesion molecules such as CD11b and CD11c, and induce the cytotoxic and migratory activities of NK cells (11–14). Moreover, transfection of the MCP-1 into human lung adenocarcinoma cells inhibited the formation of metastases, presumably via the activation of NK cells (15). It was recently reported that NK cells can mediate long-lived, Ag-specific adaptive recall responses independently of B cells and T cells (16). These observations suggest that MCP-1 can induce specific tumor immunity by enhancing NK cell functions even in this system.

Thus, we evaluated the long-term systemic immunomodulatory effects of a bicistronic recombinant adenovirus vector (rAd) expressing both HSV-tk and MCP-1 (Ad-tk-MCP1). After the primary s.c. HCC tumors in athymic nude mice were eradiated by using Ad-tk-MCP1, the same HCC cells were injected into an another site of the same mice to prove the presence of NK cell-mediated, long-term immunity. Moreover, we explored whether innate immune responses induced by NK cells were involved in these procedures. In this study, we provide definitive evidence to indicate that codelivery of a suicide gene and MCP-1 exerts prolonged NK cell-mediated antitumor effects in this model, suggesting a plausible strategy to prevent HCC recurrence.

*Department of Gastroenterology, Graduate School of Medical Science and †Division of Molecular Bioregulation, Cancer Research Institute, Kanazawa University, Kanazawa, Japan

Received for publication October 27, 2005. Accepted for publication October 13, 2006.

The costs of publication of this article were defrayed in part by the payment of page charges. This article must therefore be hereby marked *advertisement* in accordance with 18 U.S.C. Section 1734 solely to indicate this fact.

[1] Address correspondence and reprint requests to Dr. Shuichi Kaneko, Department of Gastroenterology, Graduate School of Medical Science, Kanazawa University, 13-1 Takara-machi, Kanazawa 920-8641, Japan. E-mail address: skaneko@medf.m.kanazawa-u.ac.jp

[2] Abbreviations used in this paper: HCC, hepatocellular carcinoma; AGM1, asialo GM1; BNL, BNL 1ME A.7R.1 HCC cell line; DC, dendritic cell; GCV, ganciclovir; HSV-tk, HSV thymidine kinase; MMC, mitomycin C; MOI, multiplicity of infection; rAd, recombinant adenovirus vector; Ad-tk, rAd expressing HSV-tk; Ad-tk-MCP1, rAd expressing both HSV-tk and MCP-1; Ad-MCP1, rAd expressing MCP-1; Ad-lacZ, rAd expressing lacZ; $TCID_{50}$, 50% tissue culture infectious dose.

 0022-1767/06/$2.00

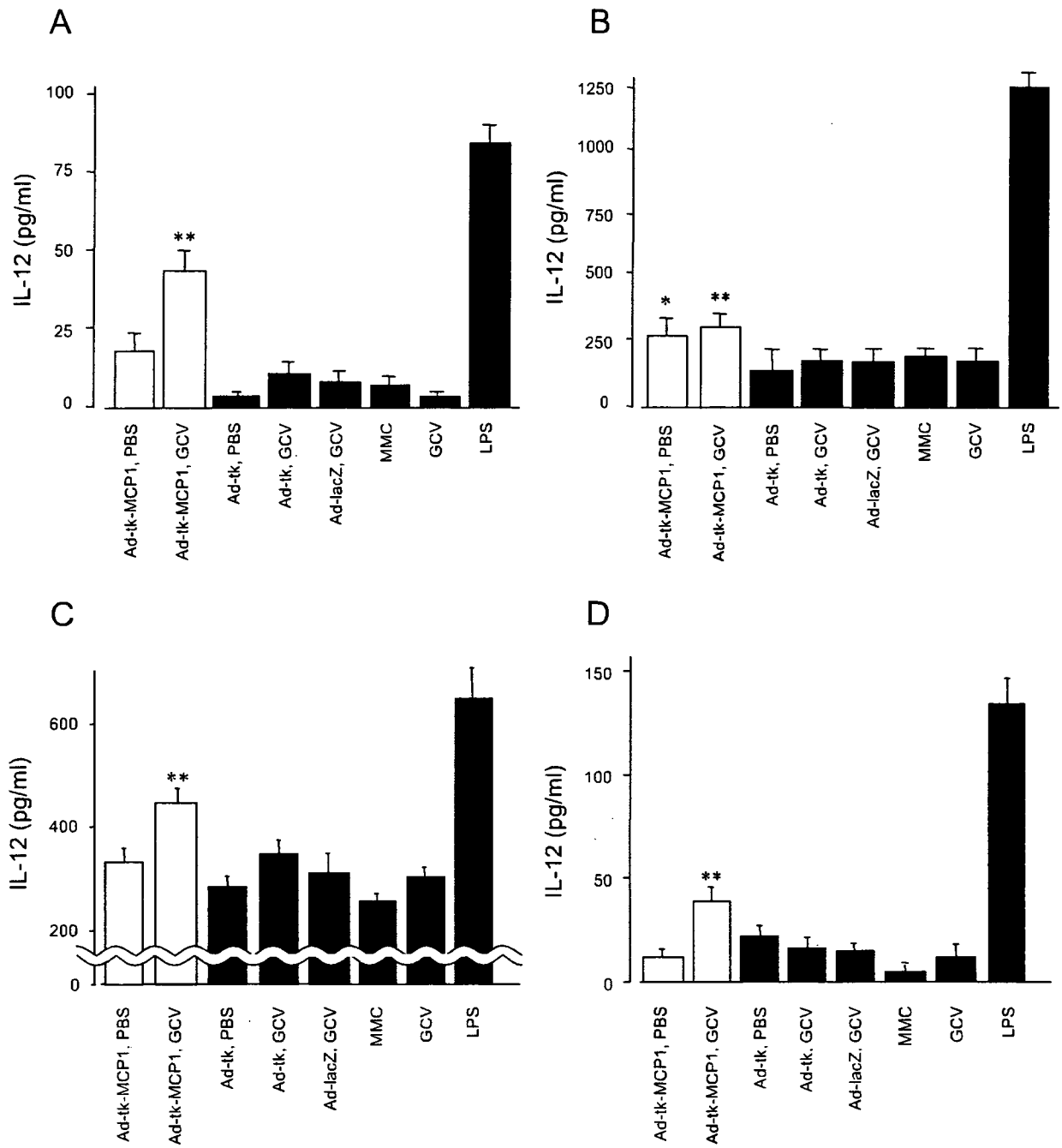

FIGURE 1. IL-12 production by monocytes and DCs cocultured with apoptotic or nonapoptotic HCC cells infected with rAds in vitro. HuH7 cells were infected with Ad-tk-MCP1, Ad-tk, and Ad-lacZ at an MOI of 5 for 24 h. Aliquots of 10^5 mouse (*A*) and human (*C*) monocytes or 10^5 mouse (*B*) and human (*D*) DCs were cocultured with 10^5 rAd- or MMC-treated HuH7 cells and treated with or without GCV for two days, and the concentrations of IL-12 in the medium were evaluated using an immunoassay. Each value is the mean ± SE of triplicate experiments. *, $p < 0.05$ compared to Ad-tk with PBS (Ad-tk, PBS); **, $p < 0.05$ compared to Ad-tk with GCV (Ad-tk, GCV) by the Mann-Whitney *U* test.

Materials and Methods

Recombinant adenoviruses

The bicistronic Ad-tk-MCP1 (10), which harbors the HSV-tk gene and the human MCP-1 gene in sequence and is driven by a CAG promoter constructed from a cytomegalovirus enhancer, a chicken β-actin promoter and part of rabbit β-globin, was prepared, purified, and titrated according to the protocols supplied by the manufacturer (Takara Bio) as described (17, 18). Briefly, using the internal ribosomal entry site (IRES) fragment of the encephalomyocarditis virus, the plasmid ptk-IRES-MCP1 (tk-MCP1) was constructed and the fragment was inserted into the cosmid vector (pAd-tk-MCP1). Ad-tk-MCP1 was subsequently generated by transfecting 293 cells with pAd-tk-MCP1 and *Eco*T22I-digested adenovirus 5-dlX DNA-terminal protein complex. The rAd expressing HSV-tk (Ad-tk), lacZ (Ad-lacZ) and MCP-1 (Ad-MCP1) were constructed in the same way (8). The rAds were purified on cesium gradients and their titers were determined by the 50% tissue culture infectious dose ($TCID_{50}$) method (19).

Cell lines and culture

The human HCC cell line HuH7 (20) and the mouse HCC cell line BNL 1ME A.7R.1 (BNL) were cultured in DMEM (Invitrogen Life Technologies)

supplemented with 10% heat-inactivated FBS (Invitrogen Life Technologies). When infected with Ad-tk-MCP1 or Ad-MCP1, BNL cells produced MCP-1 protein at similar levels as HuH7 cells (data not shown), suggesting that human MCP-1 protein was efficiently expressed in the infected human and mouse HCC cell lines.

Preparation of dendritic cells (DCs) and monocytes

Murine DCs were generated using the method of Lutz et al. (21). Briefly, bone marrow cells were harvested from 6-wk-old male BALB/c-*nu/nu* mice (CLEA Japan). Erythrocytes were lysed with ammonium chloride potassium buffer (BioWhittaker), and the nucleated cells were plated in plastic bacteriologic dishes in 10 ml of RPMI 1640 supplemented with 10% heat-inactivated FBS and 20 ng/ml murine GM-CSF (PeproTec), with the culture medium refreshed every 3 days. On day 8, the nonadherent DCs were collected. Purity was routinely >95% $CD11c^+$ DC as determined by FACS analysis.

Thioglycollate-elicited murine peritoneal exudate cells were collected as described (22). Briefly, nude mice were i.p. injected with 2 ml of 3% fluid thioglycollate medium (Wako Pure Chemical) and sacrificed 4 days later, followed by peritoneal lavage with 10 ml of cold PBS. Approximately 90% of the collected peritoneal cells were positive for both Mac-1 (CD11b) and $I\text{-}A^d$ MHC class II when stained with PE-conjugated anti-Mac-1 Ab (clone M1/70; BD Pharmingen) and FITC-conjugated $I\text{-}A^d$ MHC class II (clone AMS-32.1; BD Pharmingen).

Human monocytes and DCs were isolated from healthy blood donors (23). Briefly, PBMCs were isolated by centrifugation in Lymphoprep tubes (Nycomed). PBLs were then incubated in 6-well cell culture plates and the resultant adherent cells were collected as a monocyte population consisting of ~70% $CD14^+$ (clone MϕP9; BD Pharmingen) cells, as determined by flow cytometric analysis. The monocyte population was further grown into differentiated DCs by culturing them for 1 wk in CellGro DC medium (Good Manufacturing Practice grade; Cell Genix) supplemented with 100 ng/ml GM-CSF (Cell Genix) and 50 ng/ml IL-4 (Cell Genix). The cells were collected with viability of >80%, and >60% of cells were identified as $CD14^-HLA\text{-}DR^+$ (clone L243; BD Pharmingen) DCs.

Assays for IL-12 production in vitro

HuH7 cells were infected with Ad-tk-MCP1, Ad-tk, or Ad-lacZ at a multiplicity of infection (MOI) of 5 for 24 h. Aliquots of 10^5 DCs or monocytes were cocultured with 10^5 rAd- or mitomycin C (MMC)-treated HuH7 cells in 1.0 ml of culture medium in a 24-well tissue culture plate and treated with or without GCV for two days at 37°C. The concentrations of IL-12 in the medium were quantitated using an immunoassay kit (BioSource International).

Animal studies

The following investigations were conducted in accordance with the Institutional Animal Care and Use Committee guidelines of Kanazawa University. Six-week-old male athymic nude mice were s.c. injected with 5×10^6 HuH7 cells on day 0. On days 3 and 4, 5×10^7 $TCID_{50}$ (100 μl) of Ad-tk-MCP1, Ad-tk, or Ad-MCP1 was injected into the s.c. tumors, and the mice were treated with 75 mg/kg GCV injected into the peritoneal cavity every day for the next 5 days (days 5–9). Following complete eradication of the primary tumors, the mice were s.c. rechallenged on day 14 with 3×10^6 HuH7 cells or injected with 1×10^3 BNL cells at a distance of >3 cm from the primary challenge site. Nine of 80 (11.3%) mice treated with Ad-tk-MCP1 and 9 of 44 (20.4%) treated with Ad-tk did not show a complete eradication of the primary tumor by the final measurement and therefore were excluded from a rechallenge experiment. In some experiments, Ad-tk-MCP1-treated animals were i.p. administered 200 μl of 1 mg/ml polyclonal rabbit anti-asialo GM1 (AGM1) Ab (Wako Pure Chemical), an Ab against NK cells (24, 25), or 200 μl of rabbit serum (Sigma-Aldrich), 1 ml of 2 mg/ml carrageenan (Sigma-Aldrich), which inactivates macrophages in vivo (26–28), or 1 ml of PBS on days 11, 12, 13, 20, 27, 34, 41, and 48. In another series of experiments, Ad-tk-MCP1-treated animals were i.p. administered 250 μg of neutralizing goat anti-mouse IL-12 Ab (Sigma-Aldrich), 225 μg of anti-IL-12 Ab plus 25 μg of anti-mouse IL-18 Ab (93-10C; Medical & Biological Laboratories), or 250 μg of control IgG Ab (goat and/or rat; Sigma-Aldrich) on days 14 and 17. Tumor sizes were measured every 4 days after the second tumor injection, and tumor volumes were calculated according to the formula (longest diameter) × (shortest diameter)^2/2.

In another series of experiments, immunocompetent BALB/c-jcl mice (CLEA Japan) were s.c. injected with 1×10^5 BNL cells infected with each rAd at an in vitro MOI of 100 on day 0. GCV was administered i.p. for the next 5 days (days 1–5), and the primary tumors were completely eradicated. These mice were s.c. injected with 1×10^4 BNL cells in other sites on day 14, and the tumor sizes were measured every 7 days.

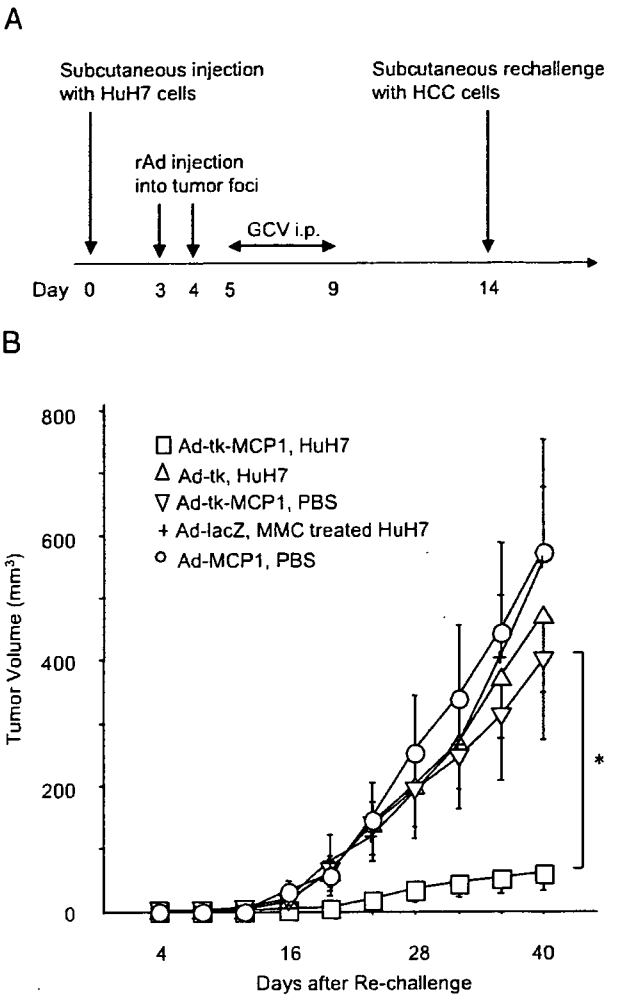

FIGURE 2. Prolonged antitumor effects of rAds expressing HSV-tk with or without MCP-1 in an athymic nude mouse model of HCC. *A*, Mice were s.c. injected with 5×10^6 HuH7 cells on day 0. On days 3 and 4, 5×10^7 $TCID_{50}$ of Ad-tk-MCP1, Ad-tk, Ad-lacZ, or Ad-MCP1 were injected into the tumors, and the mice were i.p. injected with 75 mg/kg GCV every day for the next 5 days (days 5–9). Following complete eradication of the primary tumors, the mice were s.c. rechallenged with 3×10^6 HuH7 cells at other sites on day 14. *B*, Tumor sizes were measured every 4 days. The results are the means of three independent experiments. *, $p < 0.001$ compared to Ad-tk with HuH7 (Ad-tk, HuH7) by the Mann-Whitney's *U* test.

ELISA for serum IL-12 and IL-18

Mouse sera were collected before the injection of s.c. primary tumors and after the rechallenge with tumors, and IL-12 and IL-18 concentrations were measured using immunoassay kits (IL-12 from BioSource International and IL-18 from Medical & Biological Laboratories).

Immunohistochemical analysis

Tumor tissues and spleens were resected on day 16 (2 days after tumor rechallenge). The tissue samples, except those used for F4/80 (A3-1; Serotec) staining, were embedded in OCT compound (Sakura Finetek) and snap frozen in liquid nitrogen. Cryostat sections of frozen tissues were fixed in cold acetone for 10 min, followed by rinsing three times in PBS. The tissue samples used for F4/80 staining were fixed in 10% phosphate-buffered formalin and embedded in paraffin. To avoid nonspecific staining,

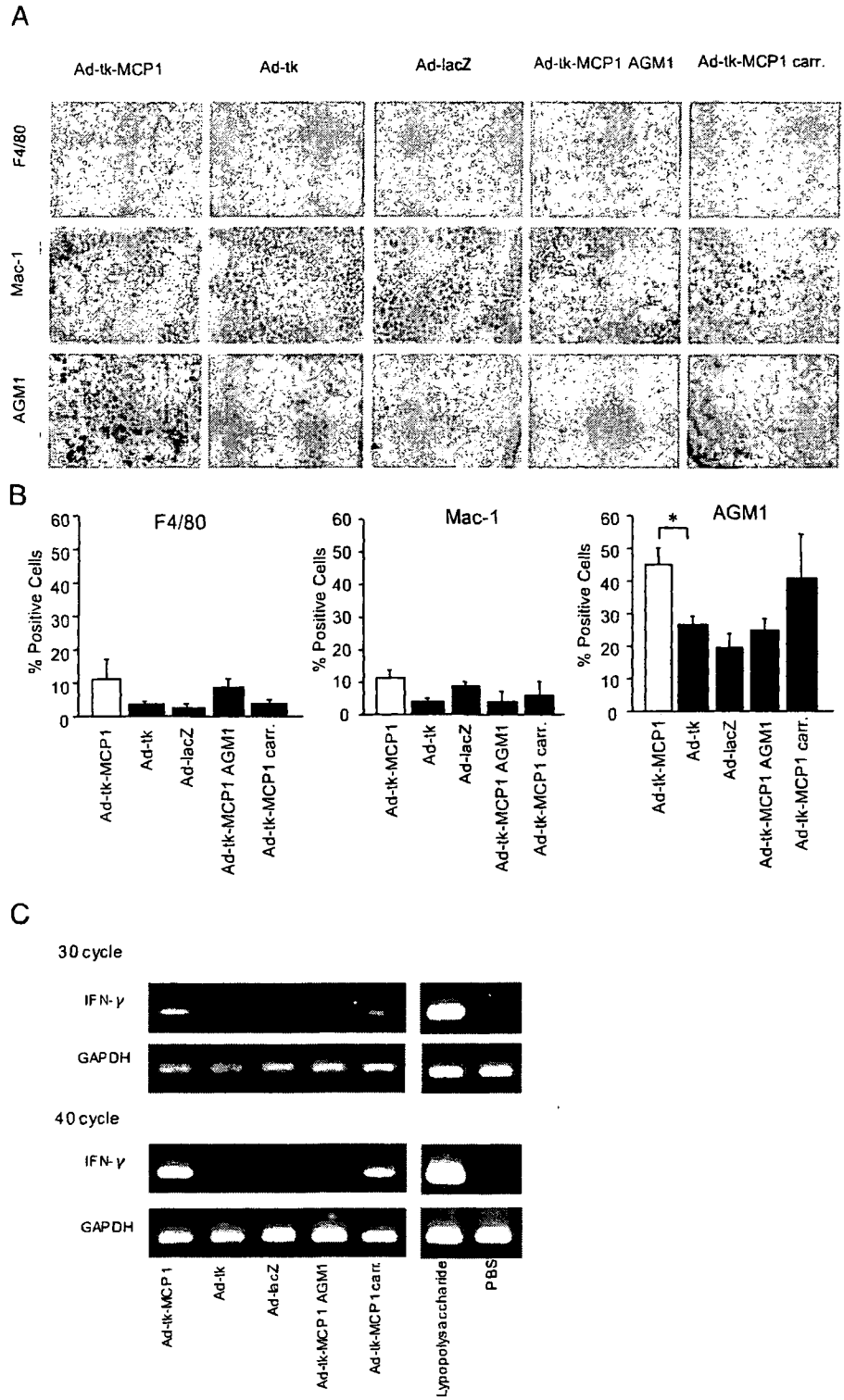

FIGURE 3. Expression of AGM1, F4/80, and Mac-1 Ags and IFN-γ mRNA in rechallenged tumor tissues. In the experiment described in the legend to Fig. 2, tumor tissues were resected 2 days after tumor rechallenge and analyzed immunohistochemically and estimated for IFN-γ mRNA expression by RT-PCR. *A*, Tumor tissues obtained from mice whose primary tumors were treated with Ad-tk-MCP1, Ad-tk, and Ad-LacZ were stained with anti-AGM1, F4/80, and Mac-1 Abs. Original magnification, ×100. *B*, Quantitative morphometric analysis showing the proportions of positive cells in areas of 100 tumor cells. Values are the means ± SE of triplicate experiments. *, $p < 0.05$ compared to Ad-tk by the Mann-Whitney's *U* test. *C*, RT-PCR were conducted in accordance with the manufacture's protocol as described in *Materials and Methods*. Bands corresponding to IFN-γ (384 bp) and GAPDH (265 bp) were detected. Splenocytes treated with 1 μg/ml LPS were used as a positive marker and tumor tissues treated with PBS were used as a negative control. carr., Carrageenan.

avidin and biotin in the tissues were blocked using a blocking kit (Vector Laboratories). The slides were subsequently incubated with Abs against AGM1, F4/80, Mac-1, CD11c (HL3; BD Pharmingen), or CD45R (RA3-6B2; BD Pharmingen) for 30 min at room temperature. Negative controls included staining with the corresponding isotype for each Ab and subsequent staining with the secondary Ab. The reactions were visualized using a VECTASTAIN ABC Standard kit (Vector Laboratories), followed by counterstaining with hematoxylin.

RT-PCR for IFN-γ gene expression

Total RNA was extracted from tumor tissues resected on day 10 using a total cellular RNA isolation kit (Ambion) according to the manufacturer's protocol. Each RT-PCR was performed using 1 μg of total RNA and an oligo(dT) adaptor primer and an RNA PCR kit (avian myeloblastosis virus), version.2.1 (Takara Bio). The amplification protocol consisted of an initial denaturation at 94°C for 2 min followed by 30 or 40 cycles of

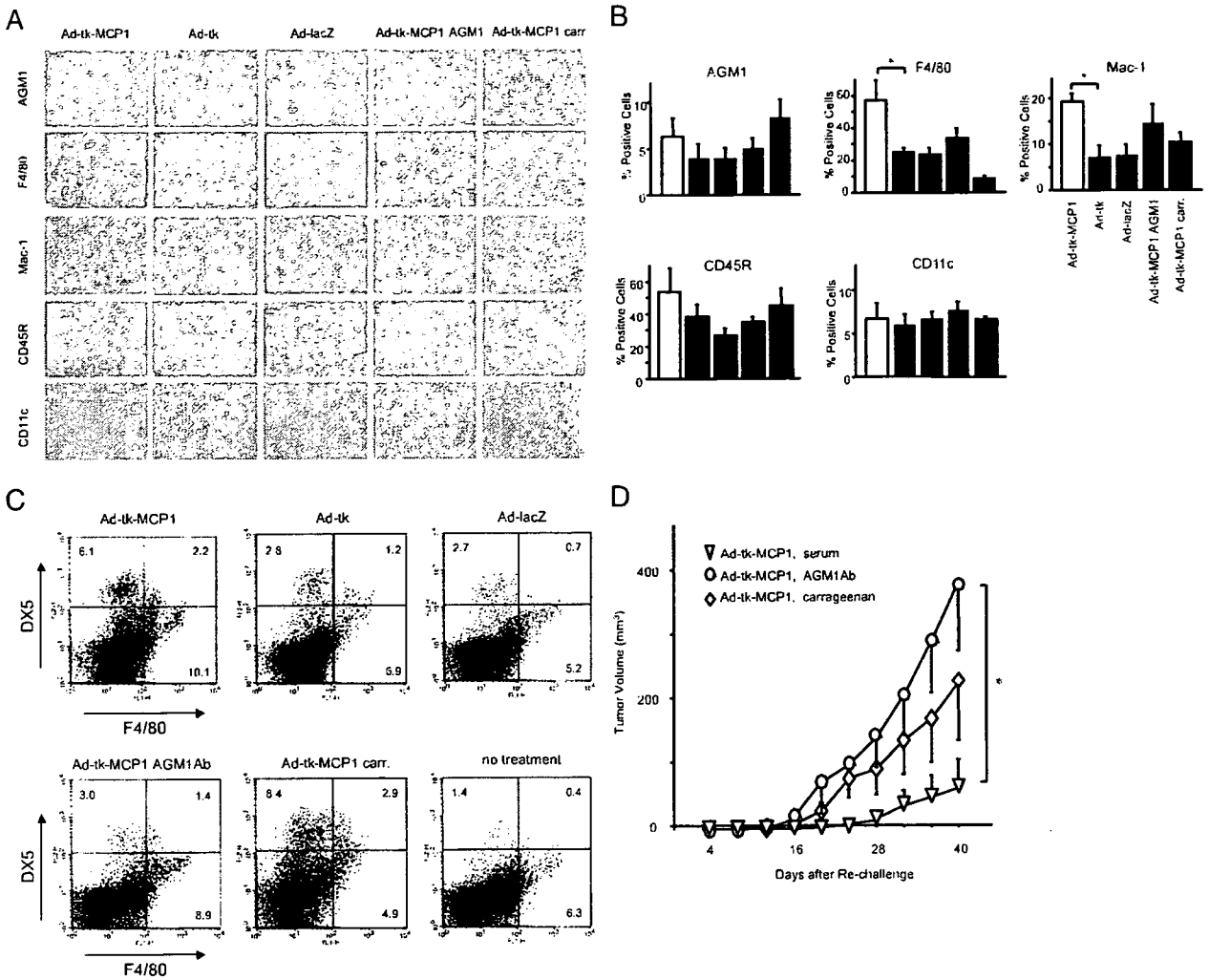

FIGURE 4. *A–C.* Immunohistochemical detection of AGM1, F4/80, Mac-1, CD11c, and CD45R in spleens. In the experiment described in the legend to Fig. 2, spleens were resected 2 days after the tumor rechallenge. *A.* The numbers of immune cells in the spleens were analyzed immunohistochemically using Abs against AGM1, F4/80, Mac-1, CD11c, and CD45R. Original magnification, ×100. *B.* Quantitative morphometric analysis showing the percentage of positive cells in 50 ×400 power fields. Each value is the mean ± SE of triplicate experiments. *, $p < 0.05$ compared with Ad-tk by the Mann-Whitney *U* test. *C.* Surface expression of DX5 and F4/80 in cell populations obtained from spleens was assessed by FACS. The results are representative of two independent experiments. carr., Carrageenan. *D.* The effects of anti-AGM1 Ab or carrageenan on the growth of rechallenged tumors. At the rechallenge with HuH7 cells, Ad-tk-MCP1-treated animals were i.p. administered with 200 μl of 1 mg/ml anti-AGM1 Ab (Ad-tk-MCP1, AGM1 Ab), 200 μl of rabbit serum (Ad-tk-MCP1, serum) or 1 ml of 2 mg/ml carrageenan (Ad-tk-MCP1, carrageenan) as described in *Materials and Methods*. Tumor sizes were measured every 4 days. The results are the means of two independent experiments. *, $p < 0.05$ compared to Ad-tk-MCP1 with PBS or serum (Ad-tk-MCP1, serum) by the Mann-Whitney *U* test.

denaturation at 94°C for 30 s, annealing at 60°C for 30 s, and an extension at 72°C for 1.5 min. The PCR primers for the mouse IFN-γ and GAPDH genes were purchased from R&D Systems.

Flow cytometry

Single cell suspensions of splenocytes were resuspended in PBS containing 1% BSA and 0.1% sodium azide and incubated for 30 min on ice with FITC-conjugated rat anti-mouse-F4/80 and PE-conjugated rat anti-mouse pan NK cells (DX5; BD Pharmingen) or with FITC-conjugated rat anti-mouse-CD4 (BD Pharmingen) and PE-conjugated rat anti-mouse CD8 (BD Pharmingen). The cells were washed, resuspended in PBS, and analyzed in a FACScan with CellQuest software.

Statistical analysis

All results were expressed as means ± SE. The statistical significance of differences between groups was evaluated by repeated measures ANOVA for the duration of the serum levels of IL-12 or the Mann-Whitney *U* test for the other results.

Results

Apoptotic HCC cells expressing MCP-1 augment IL-12 production by monocytes and DCs in vitro

IL-12, which was originally identified as an NK-stimulatory factor and a cytotoxic lymphocyte maturation factor, is one of the most promising cytokines in cancer treatment because of its multiple effects. IL-12 is produced by APCs such as macrophages, DCs, and B cells following the appropriate stimuli (29–31). To evaluate the immunomodulatory effects of rAds expressing HSV-tk with or without MCP-1 (Fig. 1), we measured IL-12 production by monocytes and DCs, both of which had been cocultured with HCC cells that had been infected with rAds (Fig. 1). Murine peritoneal exudate cells, consisting mostly of macrophages, and human monocytes cocultured with apoptotic HCC cells induced by the HSV-tk/GCV system plus MCP-1 produced greater amounts of IL-12

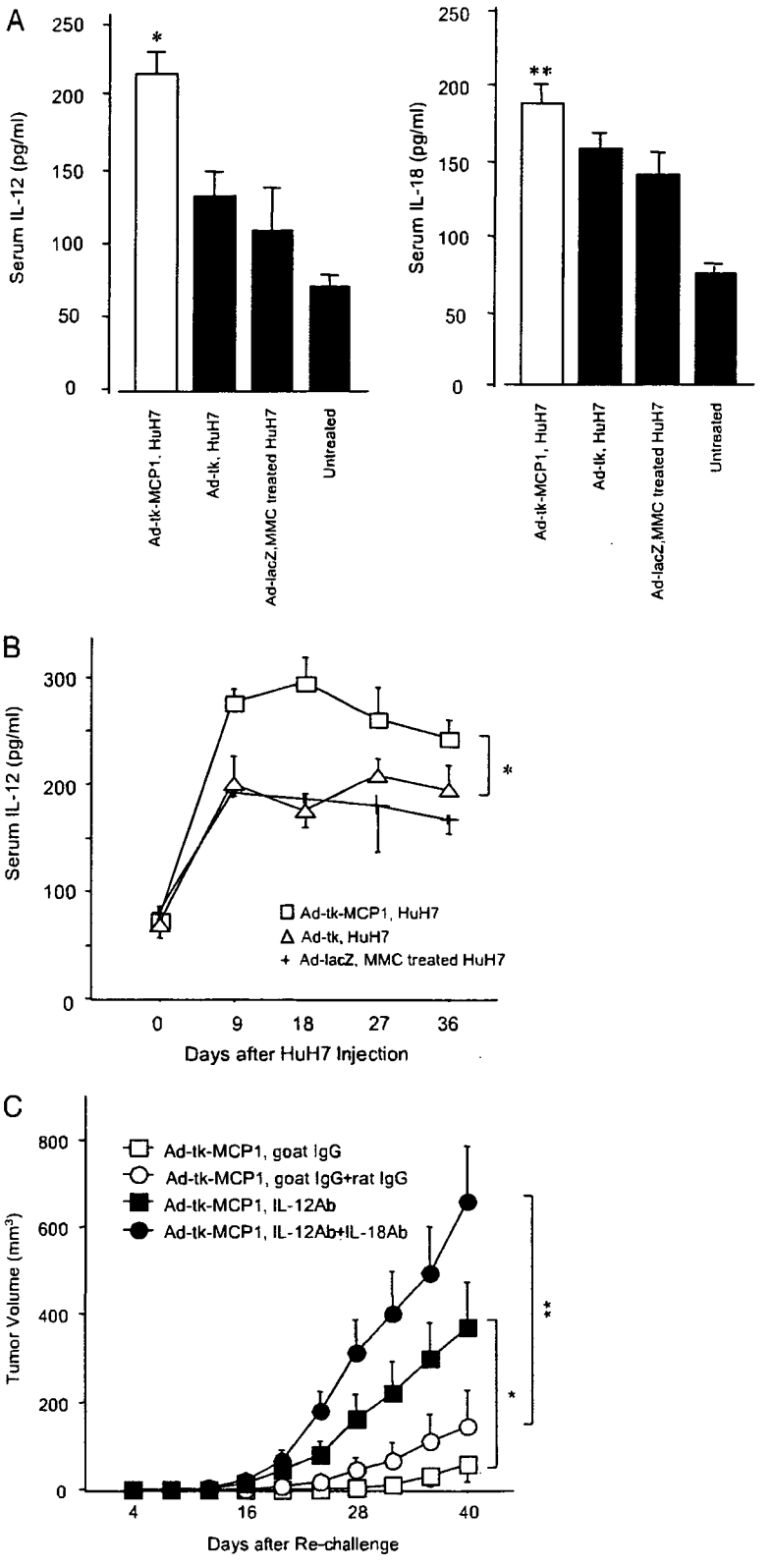

FIGURE 5. Roles of IL-12 and IL-18 in growth suppression of rechallenged HuH7 cells. *A*, Mouse sera were collected before s.c. injection of primary tumor cells (untreated) and 2 days after rechallenge with HuH7 cells, and IL-12 and IL-18 concentrations were measured using immunoassay kits. Each value is the mean ± SE of triplicate experiments. *, $p < 0.01$; **, $p < 0.05$ compared to Ad-tk by the Mann-Whitney *U* test. *B*, Serum concentrations of IL-12 were monitored every 9 days after the injection of primary tumors. Each value is the mean ± SE of triplicate experiments. *, $p < 0.05$ compared to Ad-tk with HuH7 (Ad-tk, HuH7) by repeated measures ANOVA. *C*, At rechallenge with HuH7 cells, Ad-tk-MCP1-treated animals were i.p. administered with 250 μg of anti-IL-12 Ab (Ad-tk-MCP1, IL-12Ab), 225 μg of anti-IL-12 Ab plus 25 μg of anti-IL-18 Ab (Ad-tk-MCP1, IL-12Ab+IL-18Ab), or 250 μg of control IgG Ab (Ad-tk-MCP1, goat IgG or Ad-tk MCP1, goat IgG+rat IgG). Tumor sizes were measured every 4 days. The results are representative of two independent experiments. *, $p < 0.05$ compared to Ad-tk-MCP1 with goat IgG (Ad-tk-MCP, goat IgG); **, $p < 0.01$ compared to Ad-tk-MCP1 with goat IgG plus rat IgG (Ad-tk-MCP, goat IgG+rat IgG) by the Mann-Whitney *U* test.

than did those cocultured with apoptotic HCC cells induced by the HSV-tk/GCV system alone (Fig. 1, *A* and *C*). Murine bone marrow DCs tended to produce IL-12 when cocultured with HCC cells infected with rAds expressing MCP-1 without regard to HSV-tk-induced apoptosis (Fig. 1*B*). Human DCs produced large amounts of IL-12 when cocultured with HSV-tk/GCV-induced apoptotic tumor cells, which expressed MCP-1, as did human monocytes (Fig. 1*D*). Thus, the phenomena observed in this xenograft model may also be observed under human allogeneic conditions.